

# GeantV

## Results from the prototype of concurrent vector particle transport simulation in HEP

G Amadio<sup>a</sup>, A Ananya<sup>a</sup>, J Apostolakis<sup>a</sup>, M Bandieramonte<sup>a,b</sup>, S Banerjee<sup>c</sup>,  
A Bhattacharyya<sup>d</sup>, C Bianchini<sup>e,f</sup>, G Bitzes<sup>a</sup>, P Canal<sup>c</sup>, F Carminati<sup>a</sup>,  
O Chaparro-Amaro<sup>g</sup>, G Cosmo<sup>a</sup>, J C De Fine Licht<sup>a</sup>, V Drogan<sup>a,h</sup>,  
L Duhem<sup>j</sup>, D Elvira<sup>c</sup>, J Fuentes<sup>k</sup>, A Gheata<sup>a</sup>, M Gheata<sup>a,l</sup>, M Gravey<sup>m</sup>,  
I Goulas<sup>a</sup>, F Hariri<sup>a</sup>, S Y Jun<sup>c</sup>, D Konstantinov<sup>a,u</sup>, H Kumawat<sup>d</sup>,  
J G Lima<sup>c</sup>, A Maldonado-Romo<sup>g</sup>, J Martínez-Castro<sup>g</sup>, P Mato<sup>a</sup>,  
T Nikitina<sup>a,p</sup>, S Novaes<sup>e</sup>, M Novak<sup>a</sup>, K Pedro<sup>c</sup>, W Pokorski<sup>a</sup>, A Ribon<sup>a</sup>,  
R Schmitz<sup>s</sup>, R Seghal<sup>d</sup>, O Shadura<sup>a,r</sup>, E Tcherniaev<sup>a</sup>, S Vallecorsa<sup>a,p</sup>,  
S Wenzel<sup>a</sup>, Y Zhang<sup>a,t</sup>

the date of receipt and acceptance should be inserted later

**Abstract** Full detector simulation was among the largest CPU consumer in all CERN experiment software stacks for the first two runs of the Large Hadron Collider (LHC). In the early 2010's, the projections were that simulation demands would scale linearly with luminosity increase, compensated only partially by an increase of computing resources. The extension of fast simulation approaches to more use cases, covering a larger fraction of the simulation budget, is only part of the solution due to intrinsic precision limitations. The remainder corresponds to speeding-up the simulation software by several factors, which is out of reach using simple optimizations on the current code base. In this context, the

GeantV R&D project was launched, aiming to redesign the legacy particle transport codes in order to make them benefit from fine-grained parallelism features such as vectorization, but also from increased code and data locality. This paper presents extensively the results and achievements of this R&D, as well as the conclusions and lessons learnt from the beta prototype.

**Keywords** Detector Simulation, Particle Transport, Concurrency, Parallelism, Vectorization

### 1 Introduction

With ever-increasing data acquisition rates and detector complexity, the experimental particle physics program is reaching exascale in terms of produced data. The high-luminosity phase of the Large Hadron Collider (LHC) will produce about 150 times more data than in its first run [1], hence a proportional increase in computing requirements is expected. All computing areas involved in the processing chain are expected to cope with the increased throughput, under the assumption of a flat computing budget.

Particle transport simulation, is an essential component in all phases of a particle physics experiment, from detector design to data analysis. Its main role is trying to predict the detector response after the traversal of particles, which is a very complex task involving a large number of models. Among the most used particle transport libraries in high-energy physics, we can identify Geant4 [2], Fluka [3], and Geant3 [4]. Simulation is one of the most computationally demanding applications in

<sup>a</sup>CERN, EP Department, Geneva, Switzerland  
<sup>b</sup>University of Pittsburgh, Pittsburgh, PA, 15260, USA  
<sup>c</sup>Fermi National Accelerator Laboratory, Batavia, IL, 60510, USA  
<sup>d</sup>Bhabha Atomic Research Centre (BARC), Mumbai, India  
<sup>e</sup>São Paulo State University (UNESP), São Paulo, Brazil  
<sup>f</sup>Mackenzie Presbyterian University, São Paulo, Brazil  
<sup>g</sup>Centro de Investigación en Computación. Instituto Politécnico Nacional. Mexico City. Mexico  
<sup>h</sup>Taras Shevchenko National University of Kyiv, Ukraine  
<sup>j</sup>Intel Corporation, Santa Clara, CA, 95052, USA  
<sup>k</sup>Dep. of Computer Science and Information Technologies, University of Bio-Bio, Chile  
<sup>l</sup>Institute of Space Sciences, Bucharest-Magurele, Romania  
<sup>m</sup>Univ. of Lausanne, Faculty of Geosciences and Environment, Institute of Earth Surface Dynamics  
<sup>p</sup>Gangneung-Wonju National Univ., Gangneung, South Korea  
<sup>r</sup>National Technical University of Ukraine, Kiev Polytechnic Institute, Kiev, Ukraine  
<sup>s</sup>Univ. of California, Santa Barbara, California, USA  
<sup>t</sup>KIT, Karlsruhe, Germany  
<sup>u</sup>NRC 'Kurchatov Institute' IHEP, Protvino, Russia

HEP, keeping busy more than half of the distributed computing resources of the LHC. The increasing demand for simulated data samples can in part be satisfied with approximate (so-called) fast simulation techniques, but accelerating the detailed simulation process remains essential for increasing simulation throughput.

The ambitious experiment upgrades are made in a context where computing technology is rapidly evolving. Since increasing the clock speed and shrinking the transistors became limited by quantum leakage, industry is exploring alternative solutions on the path to the next technological breakthrough. The main hardware manufacturers now favor parallel (or vector) processing units as well as heterogeneous hardware solutions with accelerators such as GPUs, FPGAs, and ASICs, allowing a performance boost for many domain-specific applications. Most high-energy physics (HEP) applications are not optimized for Single Instruction Multiple Data (SIMD) or co-processors and therefore do not make efficient use of these new resources.

The SIMD model utilizes specialized CPU vector registers to execute in parallel the same sequence of instructions for multiple data. The Single Instruction Multiple Threads (SIMT) model has the same concept as SIMD but the common code (kernel) is executed by multiple synchronous threads. The main practical difference between the two models is the length of the data vector, short in the case of SIMD, usually found on CPUs, and much longer in the case of SIMT, usually found on graphics processing units. Also SIMD requires the strict alignment of all the data to be processed into a single register, while all threads in SIMT process data in their registers. Writing vectorized applications makes it easier to later port them to co-processors that implement the SIMT model.

The benefits of SIMD and SIMT have been demonstrated for applications featuring massive data parallelism, such as linear algebra and graphics. However, bringing these vectorization techniques to complex code with significant branching presents a different type of challenge. Particle transport simulation is a very demanding HEP application having many features hostile to SIMD, including sparse memory access into large data structures, deep conditional branching, as well as long algorithmic chains and deep function call stacks per data unit (a track, representing a particle state) with low code-locality.

The GeantV simulation R&D project [5] aimed to exploit modern CPU vector units by re-engineering the simulation workflow implemented in Geant4 [2] and the associated data structures. The goal was to enhance instruction locality by regrouping data (tracks) according to the tasks to be executed, rather than executing a

sequence of tasks for the same track. The advantage of such an approach (besides the temporal locality) is that it enables new forms of data parallelism that were inaccessible before, such as SIMD and SIMT. Other computational workflows in HEP, such as reconstruction or physics analysis, could benefit from the same optimisations and we expect that the lessons learned from the GeantV R&D can be applied to these areas.

The target of the GeantV prototype was to speed-up particle transport simulation applications by a factor between 2 to 5 on modern CPUs [5], compared to Geant4 in similar conditions. We have foreseen gains from SIMD and better instruction cache locality, but also code and algorithm re-factoring. To support multi- and many-core platforms, thread parallelism has been supported by the very early versions of the prototype. Another design requirement of this study is to ensure portability to various hardware architectures. The idea is to keep the same code and preserve the ability to migrate the data model representation in a device-friendly format.

## 2 Concepts and architecture

Particle transport simulation is peculiar in terms of workflow and data access patterns. In most HEP event processing applications, the data lifetime is rather short: data is filtered and processed to produce results or derived quantities that are consumed by subsequent tasks. Commonly the same data is used as constant input by several algorithms, but rather unusual to be recursively changed while being processed. This is the case for simulation, which follows the life cycle of a *track*, representing a particle travelling through the detector. The track is the central data object used by most of the transport algorithms: geometry computations, propagation in electric/magnetic fields, or physics processes affecting the associated particle. From a computational perspective, the track represents a state taken as input and modified subsequently by a sequence of tasks, collaborating to perform a *step* that moves it from one point to another. There is a design choice in the ordering of individual steps. In the traditional design, simulation engines perform consecutive steps on a single track until it completes its transportation. To use parallelism an alternative approach is required, that performs stepping on multiple tracks, which is the basic direction taken by GeantV.

An important feature of simulation driving the application design is unpredictability: particle physics is stochastic by nature, implying that the next physics process affecting a particle has to be chosen according to probability distribution functions. One cannot pre-generate a sequence of processes, because their probabil-

ities are dependent on the material properties, affected by the geometry location and kinematic properties of the current track. Hence, the scalar (per track) data flow cannot be organized as a pipeline since the next task is generally not known a priori. The most convenient concept for handling the multitude of alternative algorithms is run-time polymorphism or virtual inheritance. Moreover, the large diversity and complexity of physics and geometry algorithms typically generate deep simulation call stacks and expensive branching logic, with a corresponding loss of computational efficiency.

The main GeantV concept is to turn around the focus from being data-centric to being algorithm-centric, making simulation SIMD and SIMT friendly. Instead of following a workflow from a track’s perspective, we define static processing stages and handle track populations being processed by each stage. This change of viewpoint helps to enhance spatial and temporal code/instruction locality, at the price of using more memory and likely worse data caching. Bundling more work together also enables more fine-grain parallelism and favours deployment to heterogeneous computing resources.

Another important exploration in the context of simulation is parallelism. Multi-threading parallelism is an important lever for making use of the full processing power of modern CPUs. Even if most HEP workflows are embarrassingly parallelizable on input data (such as individual LHC collision events), most of our applications are memory-bound and simulation is not an exception. Event-level parallelism is already in production for several years in Geant4, with very good overall scaling performance in multi-threaded mode and rather small memory overhead coming from each additional thread. The only problem is that while allowing effective use of many-core CPUs, it does not produce any increase in the throughput per thread.

Vectorization is one of the throughput-increasing acceleration techniques and becomes beneficial when the code fires a large percentage of SIMD instructions. Although compiler authors are striving to provide auto-vectorized solutions, in practice there are only a few kinds of problems for which auto-vectorization works out of the box. Auto-vectorization is more likely to be successful within confined data loops with reduced branching complexity and without any data-dependence. Since, in simulation, relatively few algorithms have natural internal loops, we can only benefit from auto-vectorization in a very limited scope. What we explore in GeantV is percolating track data into low-level algorithms, aiming to loop over this data internally. This approach requires being able to schedule reasonable data populations for each vectorized algorithm.

In this approach, data needs to be first accumulated into per-algorithm containers (“baskets” in GeantV jargon), before being processed. The algorithms need to expose a new interface to handle an input basket and provide implementations handling the basket data in a vectorizable manner. Note that the tracks coming from a single event may not suffice to fill baskets efficiently, given the complex branching of simulation code and the sheer variety of physics processes needed. One framework prerequisite is, therefore, to be able to mix tracks belonging to many concurrent events in the same processing unit.

Moving one level below, the requested track data has to be gathered and copied into the vector registers. For this to happen, we copy the data into arrays, each entry corresponding to the data of one track. In this scenario, the algorithm can be expressed as an easy to vectorize loop over C-like arrays. Scattering the algorithm output data to the original tracks completes the procedure and allows the processed tracks to be dispatched to subsequent algorithms. This schema requires a data transformation layer on top of each algorithm as shown in Fig. 1.

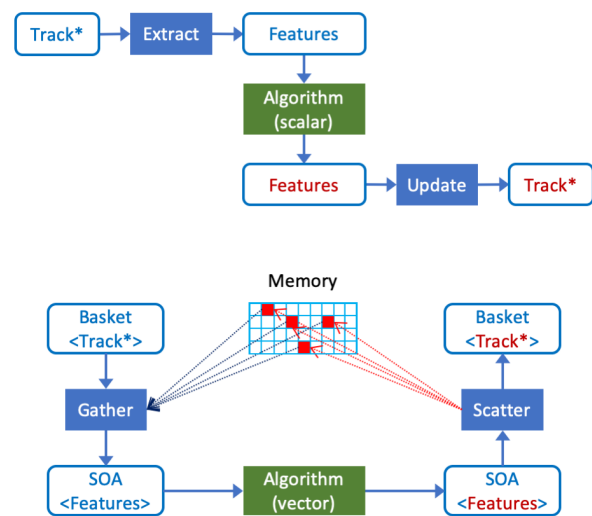


**Fig. 1** Algorithm-centric view of the operations performed for updating the track state during a single step for the scalar and vector cases.

During this study, we have thoroughly investigated available vectorization techniques in terms of programmability, performance, and portability. We evaluated auto-vectorization, compiler pragmas, SIMD libraries, and compiler intrinsics. The conclusion was that the higher the control over vectorization performance the lower the portability and programmability. Assem-

bly code or intrinsics are both difficult to write and maintain. On the other hand, auto-vectorization and compiler pragmas do not guarantee vectorization as an outcome, and this is an effect that worsens with increasing algorithm complexity. Our preferred choice was to use SIMD libraries offering a high-level approach to vectorization via SIMD types and higher-level constructs, while keeping the complexity at a reasonable level and leveraging the portability of the library. We decided to decouple as much as possible the implementation of algorithms from the concrete SIMD libraries, so we created VecCore [6], an abstraction layer on top of SIMD types and interfaces, supporting both scalar and vector backends (such as Vc [7], and UME::SIMD [8]) - the scalar backend supports SIMT as well.

## 2.1 Software design

GeantV transforms the scalar workflow into a vector one. Instead of handling one track at a time, algorithms can operate on *baskets* of tracks. Once a basket is injected in the algorithm, the vectorization problem is reduced to transforming all scalar operations on track data into vector operations on basket data. To generate efficient SIMD instructions and to quickly load data into SIMD registers, the basket data needs to be transformed from an array of track structures (AOS) to a structure of arrays of track data (SOA). This copying operation is only necessary for the part of the track data needed by the algorithm.

The workflow is orchestrated by a central run manager. This coordinates the work of several components, among which there are the event generator, the geometry and physics managers, and the user application. The main event loop can be controlled by either the GeantV application or the user framework. Primary tracks, defining the original input collision event, are either generated internally or injected by the user, being buffered by an event server. The track-stepping loop is re-entrant, executed concurrently in several threads. Each thread will take and process tracks from the event server. Once all tracks from a given event are transported, another event is generated/imported. The scheduler respects the constraint not to exceed the maximum number of events in flight set by the user.

### 2.1.1 GeantV scheduler

The scheduler's main task is to gather data efficiently in baskets for all the components, to improve vectorization. Also the multi-threaded approach needs to have good scaling to make efficient use of all available cores. During the study, we have tested several different approaches to

optimize both of these goals, and we developed several versions of the scheduler. Two of the most important workflows are presented in Appendix A.

The first version of scheduling was mostly geometry-centric, trying to benefit from observation, illustrated in Fig. 2, that many track steps are done in a smaller number of important detector volumes/materials (volume locality) with the idea that at least geometry calculations could be vectorized for such baskets. The model had a central work queue handling baskets with tracks located in the same geometry volume. Dedicated transport threads were concurrently picking baskets from the queue, transporting them to the next boundary. Whenever a track entered a new volume, it was copied into a pending basket for that volume. The worker thread that managed to fill a given basket beyond a threshold was then responsible for dispatching it to the work queue and replacing it with a recycled empty basket. A garbage collector thread was responsible for pushing partially filled baskets to the work queue whenever the queue started to be depleted. Merging produced hits and storing them to the output file was managed by a special I/O thread.

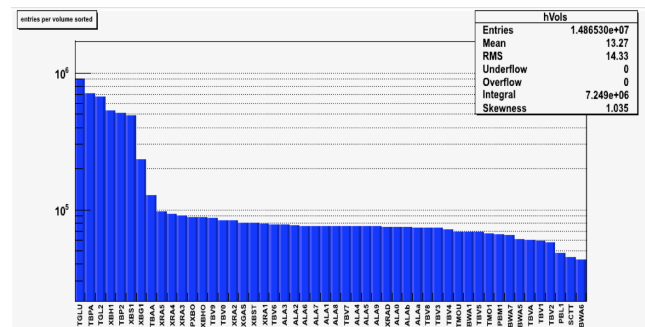


**Fig. 2** Geometry volume locality is observed in most detector simulations. This example illustrates the sorted number of simulated steps per volume in an ATLAS simulation from 2011. For this particular simulation, 50% of the steps are executed inside 50 out of 7100 logical volumes

This first approach shown in A in Appendix 1, focused on demonstrating track level parallelism with enhanced geometry locality, since vectorized algorithms for baskets were not available at the start of the project. This was an extremely useful step for understanding the changes and peculiarities of the basket-based track workflow compared to the single track approach. However, the model had scaling issues due to high contention on specific baskets and frequent flushes done by the garbage collector during the event tails.

A second version of the scheduler, shown in 27 in Appendix 1, introduced support for explicit SIMD vectorization. The basket contained a track structure of

arrays (SOA) with aligned arrays ready to be copied into the vector registers. Track data was copied in and out of the SOA, as tracks were passing from one basket to another. A simplified tabulated physics model was available in this version and, since it was not vectorized, the scheduler was still dealing only with geometry-local baskets. The prototype complexity increased and several tuneable parameters were introduced in an attempt to implement an adaptive behavior, optimizing the performance of different setups and in different simulation regimes. Gathering and scattering data into the SOA baskets introduced new overheads due to extra memory operations, plus extra bottlenecks in the concurrent approach. We tried to minimize the cost of memory operations by introducing non-uniform memory access (NUMA) awareness in handling basket data, leading to improvements of up to 10% of the simulation time.

The final version of the GeantV scheduler is shown in Fig. 3. In addition to fixing many of the previous versions' issues, such as contention in multithreaded mode and memory behavior, this version introduced a generic model for basketizing, relying on the fact that more vectorized algorithms were available, in addition to geometry ones. The new framework significantly improved the basketizing efficiency, while also accommodating scalar and vector processing flows, switching from one to another depending on the workflow conditions.

### 2.1.2 Scalar and vector workflows

To support both scalar and vector workflows in the same framework, we introduced a common interface class called *handler*, wrapping all simulation algorithms in a common tasking system. The algorithm needs to implement the appropriate scalar and vector interfaces taking as input either a single track pointer or a vector (basket) of tracks. The vector method acts as a dispatcher for the SIMD version of the algorithm: it has to first gather the needed data from the container of tracks and copy it into a custom SIMD data structure. For example, geometry navigation requires only the track positions and directions, while magnetic field propagation needs also the charge, momentum, and energy. The SIMD structure is then passed to the vectorized algorithm. The newly produced track state variables are then scattered to the original track pointers. To feed such *handlers* in a workflow, tracks executing the same algorithm need to be gathered in SIMD baskets before being handed to the vector interface. In the case of vectorization of a given algorithm is not implemented or inefficient, the scalar interface can be directly invoked, following a scalar pipeline for this algorithm.

Algorithms of the same type are grouped into *simulation stages*. The simulation stages refer to specific operations having to be executed in a pipelined manner to perform a single step moving a particle from one position to the next. The sequence of stages executed per step by baskets of tracks can be followed in Fig. 4. At the beginning of the step, a *PreStep* stage initializes the track flags and separates killed tracks handling them to a final *SteppingActions* to be accounted and scored. The remaining tracks enter the stage *ComputeIntLen* allowing the sampling of physics processes' cross-sections and the proposal of an interaction length. Subsequently, a *GeomQuery* stage computes the geometry stepping limits in the current volume and a *PrePropagation* stage uses the actual step to pre-compute if multiple scattering will affect the current step. The actual track propagation is performed during a *PropagationStage*, having one handler for neutral and one for charged particles. The multiple scattering deflection is added after the propagation in a *PostPropagation* stage, and any continuous processes are subsequently applied by the *AlongStepAction* stage. For steps limited by physics processes, a *PostStepActions* stage is executed, then the final *SteppingActions* stage that does the accounting for stopped tracks and executes user actions. Every stage has an input basket per thread, used to execute the stage in either scalar mode, by looping over the contained tracks, or in vector mode, by passing the full basket to the interface.

The workflow is executed in the following manner. Each thread collects a set of primary tracks in a special buffer, called *StackBuffer*, which emulates the functionality of a typical track stack (also used in Geant4). Secondary tracks of a higher generation are also pushed into this buffer, but prioritized compared to their ancestors. The workload manager will only copy the highest generation tracks into the basket of the first stage, then execute it. Once processed, the tracks are copied to the input basket of the second stage, and so on. Each stage has one or more follow-ups, so most particles get pushed along the stepping pipeline, but some particles may loop between stages before being able to execute the complete step. As an example, charged particle propagation requires repeated queries to the geometry to finally cross the volume boundary. The stepping loop just pushes the input buffers executing the stages one after another, multiple times, until the baskets are empty. It then takes a new bunch of tracks from the *StackBuffer*. During this loop, some tracks typically end-up in as-yet unscheduled SIMD baskets, but a subsequent loop can fill these SIMD baskets and flush them back into the pipeline.

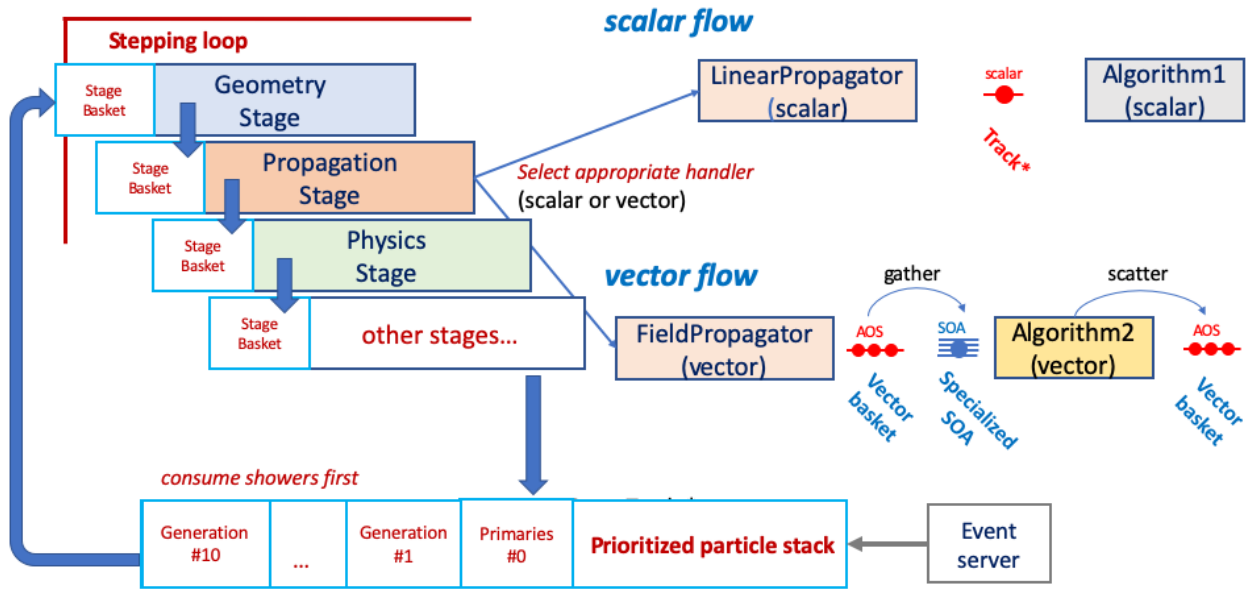


**Fig. 3** The final version of GeantV scheduler, accommodating both scalar and vector processing flows. Track data is described as a POD structure and pre-allocated in contiguous memory blocks. Each thread takes pointers to primary tracks from an event server, storing them in an input buffer (a prioritized particle stack). The stepping loop is implemented as a sequence of stages, each implementing a specific part of the processing required to make a single step for a population of tracks. Pointers to tracks tagged to execute a given stage are accumulated in the input *stage basket*, processed by the stage algorithms, then dispatched to the input stage basket of the follow-up stage. This makes a stepping pipeline for track populations. The scheduler takes bunches of track pointers (last generations first) and copies them in the *input basket* of the first stage, triggering the pipeline execution. The stage basket is dispatched internally to specific handlers of specific processing tasks: for example the propagation stage dispatches all neutral tracks to a linear propagator and the charged ones to a field propagator. The handlers of vectorized algorithms first accumulate (basketize) enough tracks to make the algorithm execution efficient. Subsequently, only the members of the track structure needed by the algorithm are gathered in the form of a structure of arrays (SOA) before being processed, then the results are scattered back to the original track pointers. Scalar algorithms make use directly of the stage basket track pointers, without having to gather/scatter data, so scalar and vector workflows can coexist. The last stage in the stepping pipeline implements the final stepping actions and calls the user application for scoring, before completing the cycle by copying the surviving tracks back to the prioritized particle stack. The scheduler has the role to push tracks in the stepping pipeline until exhausting the initial track population, then refilling it from the event server. Globally, the scheduler has also to balance the workload among concurrent threads and enforce policies to optimize the global workflow.

### 2.1.3 Concurrency model

The GeantV prototype implements parallelism at the track level. It supports an internal mode where the workload is parallelised among threads managed by the GeantV scheduler, and an external mode implemented as a call to a re-entrant task transporting an event set, where the parallelism is decided by the caller framework.

Primary tracks produced by an event generator are stored in a concurrent event server and delivered to worker threads in bunches of customized size. The track data storage itself is pre-allocated to avoid dynamic memory management, partitioned per NUMA domain, and only pointers to tracks are delivered via the event server interfaces, as shown in Fig. 5. Once a thread picks

up a set of primary tracks, it becomes the only user of the track for the given step. Due to this design, there is no synchronization needed when changing the state of a track. Threads handle tracks in their buffers; however they share a single set of SIMD baskets per NUMA domain, so a thread may steal the tracks accumulated in these baskets by other threads. Even in scalar mode, when the SIMD baskets are empty, there is a mechanism allowing threads to steal tracks from each other as a mechanism of work balancing during the processing tail at the end of events.

The concurrency model was designed to minimize the synchronization needs and reduce contention on the concurrent services, while sharing track data to increase basket populations. To handle the state of the different

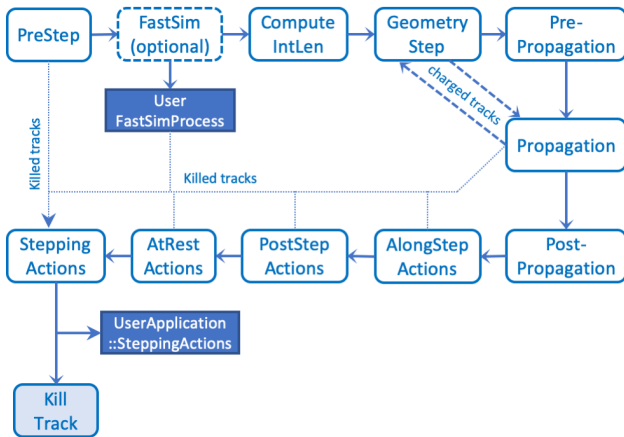


**Fig. 4** The sequence of stepping stages for baskets of particles in the GeantV prototype. Stages are connected in a predefined sequence similar to the stepping approach in Geant4, but there are also shortcuts or back connections allowing dumping stopped particles or repeating some stages. Each stage provides scalar and, in most cases, vector handlers for the stage algorithms.

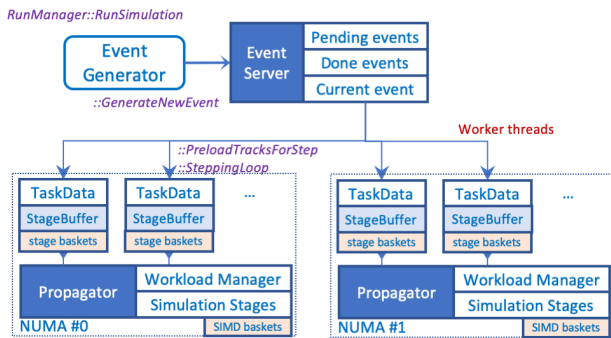


**Fig. 5** Schematic view of parallelism for the GeantV prototype. Multiple transportation tasks, handling their task data, share a set of propagator objects, one per NUMA domain. Each propagator shares a set of simulation stages with their SIMD baskets, but each transport task will handle its stack buffer of tracks. The system threads are scheduled by the run manager, and they will pick-up a free task data object from a concurrent queue. Each transport tasks will preload tracks from a concurrent event server, executing the stepping loop.

actors involved in track propagation, we embed this state in task-specific data objects, that are percolated as arguments in the calling sequence of many internal methods. This task data whiteboard is provided also to the user codes that can publish their own thread-local data structures.

To maximize the basket population, vectorized handlers have a common SOA basket shared between threads. This was a requirement for enhancing the vector population but has a large cost of increased contention and loss of data locality. To improve we have created

thread-local copies of SIMD basket for the handlers with the largest population of tracks, such as those for field propagation and multiple scattering. For these, the track population in a single thread is enough to fill them, without workflow perturbation or basket population loss. This allowed a large reduction in contention in the multi-threaded basket mode.

An important feature for fine-grained workflows is load balancing. The GeantV workflow is naturally balanced by the event server, which acts as a concurrent queue. The main problem occurs with the track depletion of the stack buffers of each thread when most of the remaining particles reside in SIMD baskets that do not have a large enough population to execute efficiently in vectorized mode. Such a regime becomes blocking when the number of events in flight has already reached the maximum specified by the user, so the scheduler enters the so-called *flush mode*. All SIMD baskets are simply flushed and the scalar *DoIt* methods are executed by the first thread triggering this mode. Flushed particles are gathered in the stage baskets of this thread, which feeds the thread but depletes, even more, the other threads that were already starving. This unbalancing mechanism is compensated by a round-robin track sharing mechanism, that allows threads to feed not only from the event server, but also from the shared buffers of other threads. To preempt the depletion regime, threads always share a small fraction of their own track populations, but will consume it themselves if no other client has. This mechanism of weak sharing allows the reduction of contention in the normal regime. Sharing is dominant during event tails and is also more important when running with many threads.

The externally-driven concurrency mode is the so-called *external loop mode*. In this mode, no internal threads are launched. The run manager provides an entry point that is called by a user-defined thread and that takes a set of events coming from the user framework. This will subsequently book a GeantV worker to perform the stepping loop, and will notify the calling framework via a callback. An example is provided, performing a CMS simplified simulation steered by a toy CMSSW [9] framework, mimicking the features of a full multi-threaded software framework of an LHC experiment. The GeantV simulation can be wrapped behind a TBB (Threading Building Blocks, Intel<sup>®</sup>) task and executed in a complex workflow, as described in Section 5.2

### 3 Implementation

This section describes the core components of GeantV libraries and modules: VecCore, VecGeom, VecMath,

propagation in a magnetic field and electromagnetic (EM) physics. Auxiliary modules, such as I/O and user interface, are briefly summarized as well.

### 3.1 Vector libraries: VecCore

Portable and efficient vectorization is a significant challenge in large scale software projects such as GeantV. The VecCore library [6] was created to address the problem of lack of portability of SIMD code and unreliable performance when relying solely on auto-vectorization by the compiler. VecCore allows developers to write generic computational kernels and algorithms using abstract types that can be dispatched to different backend implementations like the Vc [7] and UME::SIMD [8] libraries, CUDA and scalar. VecCore provides an architecture-agnostic API, illustrated in Fig 6, that covers the essential parts of the SIMD instruction set, such as performing arithmetic in vector mode, computing basic mathematical functions, operating on elements of a SIMD vector, and performing gather and scatter, load and store, and masking operations. Code written using VecCore can be annotated for running on GPUs with CUDA, and can be portable across ARM, PowerPC, and Intel architectures, if not relying on features specific to a particular backend (e.g. using CUDA-specific variables such as thread and block indices, or calling external library functions that may be available only on the CPU).

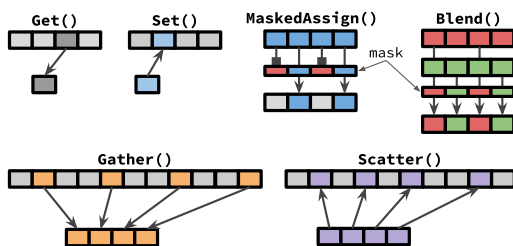


**Fig. 6** Illustration of VecCore API operations.

VecCore is used to implement vectorized geometry primitives in VecGeom (described in section 3.2), and vectorized physics models in GeantV. A brief discussion of VecCore with code samples can be found in [6], and examples of VecCore usage within VecGeom and GeantV appear in the following sections as well.

## 3.2 Geometry description: VecGeom

### 3.2.1 Introduction

Detector simulation relies on the availability of methods to describe and construct the detector layout in terms of elementary geometry primitives, as well as on interfaces that allow the determination of positions and distances with respect to the constructed layout. Well-known examples of such geometry modellers are the Geant4 geometry module and the TGeo/ROOT library. Both enable users to build detectors out of hierarchical descriptions of (constructive) solids and their containment within each other.

The geometry package, named *VecGeom*, was chosen as one of the first areas of investigation in order to study the feasibility of optimal usage of SIMD and SIMT paradigms of passing around vector data between algorithms, this being one of the main targets of GeantV. From this point of view, the primary development focus was on implementing algorithms capable of operating on elements of baskets in parallel. This signifies at the lowest level of algorithms that geometry primitives such as a simple box should offer kernels that calculate distances for a group of tracks in one function call, in addition to the normal case where only one track is handled. Mnemonic code in below shows a typical function of a geometry primitive illustrating the introduction of new vector/basket interfaces.

```
class Box // interface for a single track double Distance-
ToIn(Track) const;
// interface for multiple tracks VectorOfDoubles Distance-
ToIn(VectorOfTracks) const; ;
```

Moreover, the layout of data structures and algorithms in VecGeom should enable efficient operation in heavily multi-threaded frameworks. For instance, from a clear separation of state and services frequent track or context switches will be possible in the navigation module, which is responsible for predicting where a track will go in the geometry hierarchy along its straight-line path. Multi-platform usage was targeted since the beginning: the same code base should compile and run on CPUs as well as GPU accelerators.

Besides these primary goals, the development of VecGeom was guided and influenced by other requirements and circumstances. The first is that VecGeom should still offer traditional interfaces operating on the single-particle (scalar) level. This ensures backward compatibility with the Geant4 or TGeo systems and is, in any case, needed to treat particles that have not been put into a basket. Secondly, another geometry project called USolids [10], funded by the EU AIDA project, was already in place, with the goal to review and modernize the algorithms of Geant4 and TGeo and to unify

the geometry code base. It made sense to join forces with the USolids project in order to better use available resources. As a consequence, VecGeom was factored out into a standalone repository and its evolution could be independent of GeantV. It should be possible to serve GeantV, with a basketized treatment and GPU support, as well as making the modernized code available to clients in traditional scenarios using the single-particle interface.

The multitude of use cases and APIs to support (scalar, basketized, CPU-GPU) poses a danger of code duplication. In order to keep this minimal, VecGeom started with an approach, adopted by most GeantV modules, in which standalone (static) templated algorithmic kernels are instantiated multiple times with different types and specializations behind the public interfaces. This development architecture is visualized in Fig. 7, where the typical use cases are depicted as functional chains of algorithms (scalar, vector, GPU), all implemented in terms of the same kernel templates. In order to make this happen, the kernels need to be written in a way that they can be instantiated with native C++ types as well as with SIMD vector types (as offered by vectorization libraries such as Vc, available through VecCore). Furthermore, all constructs used should have the proper annotation to compile on the GPU (using CUDA). VecCore, prototyped within the VecGeom effort, provides the necessary abstraction that allows us to write these generic kernels.

Using this development approach, VecGeom has evolved into a geometry library that offers similar features to classical Geant4 geometry or TGeo for transport simulation for single particle queries. On top of this, the added benefit is that these algorithms are also made available for basket queries or for execution on CUDA GPUs. In particular, all major geometry primitives have been implemented and hierarchical detectors can be constructed from them via composition and placement. To solve complex geometry tasks typically needed in particle detector simulation, such as determining the minimum distance of particles to any other material

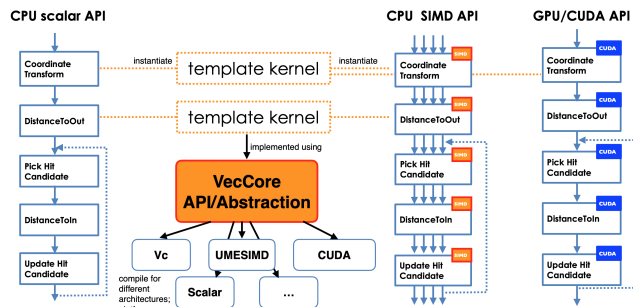


Fig. 7 Code organization; Motivation for VecCore.

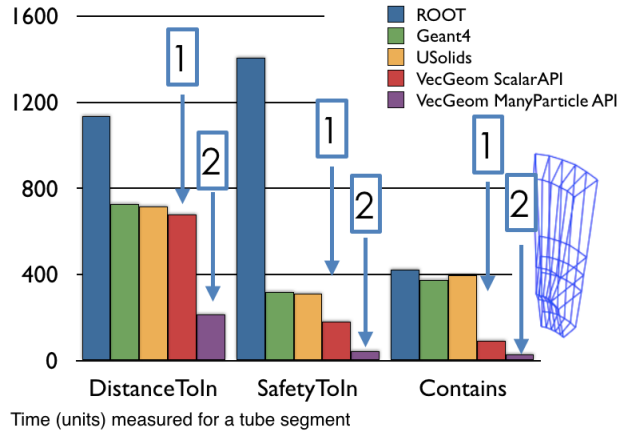


Fig. 8 Performance examples of VecGeom on the shape level for the case of a more elementary solid primitive, a tube segment. This demonstrates the performance improvement of important functions for the one-particle interface (1) (better algorithms) as well as an additional SIMD acceleration for the basket interface (2), automatically obtained from instantiating the same underlying kernel with Vc vector types.

boundary or computing the intersection points with the next object along the particles’ straight-line path, VecGeom offers navigator classes that operate on top of these primitives.

Today VecGeom’s objective is to be a high-performance library for these tasks *in general*. A lesson learned in the development was that it is worth taking a more loosely defined approach to achieving good performance and to benefit from SIMD instructions. In particular, VecGeom targets both basketized (or horizontal) vectorization as well as inner-loop (vertical) vectorization depending on the complexity of the algorithm. One can regard a simple box primitive as an example for the former and a complicated tessellated shape as an example for the latter. The best SIMD performance for a box is obtained in with the use of baskets, yet a SIMD speedup for the tessellated solid is available even in scalar/single-particle mode and does not require basket input. However, processing baskets can still be beneficial due to positive cache effects.

VecGeom has been discussed and presented in various publications [11,12,13]. In the following, we briefly review a few important results on specific aspects of VecGeom.

### 3.2.2 The performance of geometry primitives

Geometry primitives (or solids) are, besides affine transformations, the basic building blocks of complex detectors. The range goes from simple structures such as box, tube and cone, to more complex entities such as polycone, polyhedron and tessellated solids (see, e.g., the

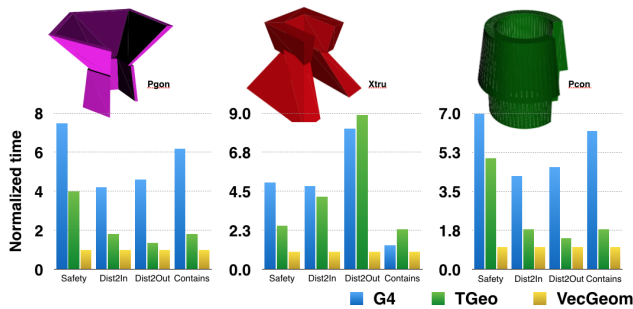


**Fig. 9** Performance speedups of more complex primitives (polycone, extruded solid, polyhedron) for scalar interfaces, compared with Geant4 and TGeo. Speedups are averages over all such solids found in the ALICE detector. In these complex cases, no additional basket SIMD acceleration is feasible.

GDML reference manual [14] for a description). In general, VecGeom offers improved performance of the solid algorithms with respect to previous implementations in Geant4 and TGeo and even with respect to USolids [10]. In most cases the improvement is due to better algorithms, often as a natural consequence of the effort to restructure towards SIMD friendly code. In the case of simpler geometry primitives, the implementations provide real SIMD acceleration for basketized usage. Figure 8 exemplifies this for a tube segment, where the SIMD acceleration was found to be of the order of 2 or better with the AVX instruction set (maximum of 4 vector lanes) via the use of VecCore and Vc.

For the more complex solids, some performance improvements for the scalar interface are shown in Fig. 9. In these cases an additional SIMD acceleration for the basket interface is not feasible due to divergent code paths taken by different particles in a basket. However, as mentioned, we can often still utilize the vector units by vectorizing inner loops or inner computations. This technique is used heavily in the tessellated solid, polyhedra and multi-union [12] and contributed to the excellent performance gain compared to previous implementations.

### 3.2.3 The performance of navigation algorithms

Apart from solid primitives, VecGeom offers navigation algorithms for solving geometry problems such as distance calculations between particles and geometry boundaries in composite geometry scenes made up of many primitives. These navigation algorithms are the primary point of contact or interface of the geometry to the simulation engine. The algorithmic chain in Fig. 7 is a simplified example of a typical navigation algorithm flow. This chain contains coordinate transformations of global particle coordinates to the frame of reference of the volume in which the particle is currently situated,

and performs distance queries to the solids embedded in this volume.

Just as with the geometry primitives, complexity defines the performance scenario for SIMD acceleration.

1. **Simple geometry limit:** In this case the current volume contains only a few (simple) solids, e.g. in simple showering modules in calorimeters.

In this limit, SIMD accelerated geometry navigation of a basket is feasible for GeantV because most of the algorithmic chain can process baskets efficiently. Table 1 gives a few benchmark numbers that show the basket-SIMD gain for simple volumes. In the generic case, the gain is rather modest because the SIMD throughput is limited by some non-vectorizable parts. However, we developed a process [13] by which we can auto-generate code implementing specialized navigators that take into account the specific properties of the geometry directly in the code. This generated code can reduce non-vectorizable parts significantly. This increases the basket-SIMD gain, but is also beneficial in its own right to improve the performance of the scalar interface. The drawback of specialized navigators is that they require some generation workflow to be run before simulation and so far they have not been extensively tested within GeantV. This explains, in part, why the overall gain from basket treatment in the current version of GeantV did not materialize for geometry navigation.

2. **Complex geometry limit:** In this case the current volume contains many solids, which is typically the case for container volumes inside which many other modules are placed.

In this limit, due to the large number of geometry objects to test, typically acceleration structures are used to reduce the complexity from  $O(N)$  to  $O(\log(N))$ , in case of hit-detection/ray-tracing, where  $N$  is the number of geometry objects present in this volume. This, in turn, makes it difficult to achieve a coherent instruction flow for all particles in a basket and to avoid branching. However, as for the tessellated solid, the navigation algorithms can benefit from SIMD acceleration via internal vectorization. In Ref. [13], a particular *regular* tree data structure, based on bounding boxes, was proposed, which can be traversed with a SIMD speedup. The VecGeom implementation for tessellated solids and for navigation are based on the same data structure. Table 2 shows a comparison of the performance of running the navigation algorithms in given complex volumes using Geant4, TGeo, or VecGeom navigator algorithms. The benefits of SIMD speedup is highlighted by the additional gain when switching from SSE4 to AVX2 instructions on the x86\_64 architec-

**Table 1** Timings to navigate a batch of test particles in selected volumes of the CMS detector. The time is dominated by the `ComputeStep` navigation interface of VecGeom in both the single-particle and basket (vector) mode. The test is done using the generic (normal) implementation of the navigator algorithm as well as with specialized generated code that is tailored to the specific volume in question. We observe that there is a small SIMD acceleration for baskets in simple volumes. This SIMD benefit can be enhanced with specialized navigators. In case of complex volumes (with many containing other volumes), there is no SIMD acceleration due to basket treatment.

Volume	type	normal scalar	normal vector	specialized scalar	specialized vector
HVQX	simple	12.6	10.6	6.4	4.7
ZDC_EMFiber	simple	10.1	8.8	5.9	2.6
ZDC_EMLayer	complex	27.0	27.0	19.7	19.3

**Table 2** Timings (in seconds) to process all test rays for a list of complex detector volumes. The worst timing is shown in red while the best in blue. VecGeom’s SIMD enabled navigation performs consistently better than any existing solutions.

Volume	#daughters	Geant4	TGeo	VG (SSE4.2)	VG (AVX2)
ALIC (ALICE)	65	0.74	1.07	0.30	0.23
TPC_Drift (ALICE)	641	14	2.2	1.2	0.9
MBWheel.1N (CMS)	789	0.84	1.09	0.49	0.35

ture. From internal vectorization, this benefit is also available in non-basketized modes.

There are many possible layouts of acceleration structures with SIMD support. This gives room for further improvement by selectively choosing the best possible acceleration structures for any given geometry volume. In this respect, VecGeom is ready to interface to kernels available from industrial ray-tracing libraries, such as Intel Embree [15,16], which has SIMD support.

### 3.3 VecMath

VecMath is a library that collects general-purpose mathematical utilities with SIMD and SIMT (GPUs) support based on VecCore. Templated fast math operations, pseudorandom number generators and specific types (such as Lorentz vectors) were initially extracted from GeantV, then developed and extended within VecMath. The library is being extended to support vector operations for 2D and 3D vectors, and general-purpose vectorized algorithms. VecMath is intended as a core mathematical library, free of external dependencies other than VecCore, usable by vector-aware software stacks.

#### 3.3.1 Fast Math

The `Math.h` header in the VecMath library contains templated implementations for `FastSinCos`, `FastLog`, `FastExp`, and `FastPow` functions. The functions can take either scalar or SIMD types as arguments. While the scalar specializations redirect to the corresponding `Vdt` [17] implementations, the SIMD specialization is currently implemented based on `Vc` types.

#### 3.3.2 Pseudorandom number generation

The VecRNG of VecMath provides parallel pRNGs (pseudorandom number generators) implementations for both SIMD and SIMT (GPU) workflows via architecture-independent common kernels, using backends provided by VecCore [6]. Several state-of-the-art RNG algorithms are implemented as kernels supporting parallel generation of random numbers in scalar, vector, and CUDA workflows. For the first phase of implementation, the following representative generators from major classes of pRNG were selected: MRG32k3a [18], Random123 [19], and MIXMAX [20]. These generators meet strict quality requirements, belonging to families of generators which have been examined in depth [21], or have evidence from ergodic theory of exceptional decorrelation properties [20]. All pass major crush-resistant tests such as DIEHARD [22] and BigCrush of TestU01 [23]. In addition, we took into consideration constraints in size of the state and performance: 1) a very long period ( $\geq 2^{200}$ ), obtained from a small state (in memory), 2) fast implementations and repeatability of the sequence on the same hardware configuration, 3) efficient ways of splitting the sequence into long disjoint streams.

The design choice for the class hierarchy was the exclusive use of static polymorphism, motivated by performance considerations. Every concrete generator inherits through the CRTP (curiously recurring template pattern) from the VecRNG base class, which defines mandatory methods and common interfaces. The implementation of VecRNG is implemented exclusive in header files, and provides a minimal set of member methods. This approach allows more flexibility in the higher

level interfaces for specific computing applications, but minimizes the overhead in compilation time.

The essential methods of VecRNG interfaces are `Uniform<Backend>()` and `Uniform<Backend>(State_t& s)`, which generate the backend type of double-precision u.i.i.d (uniformly independent and identically distributed) in  $[0,1)$ , and update the internal `fState` and the given state `s`, respectively. The `State_t` is defined in each concrete generator and provided to the base class through `RNG_traits`. One of the associated requirements for each generator in VecRNG is to provide an efficient skip-ahead algorithm,  $s_{n+p} = f_p(s_n)$  (i.e., advancing a state,  $s_n$  by  $p$  sequences, where  $p$  is the unit of the stream length or an arbitrary number) in order to assign disjointed multiple streams for different tasks. For example, the mandatory method, `Initialize(long n)`, moves the random state at the beginning of the given  $n^{\text{th}}$  stream. Each generator supports both scalar and vector backends with a common kernel. `Random123` has an extremely efficient stream assignment without any additional cost since the key serves as the stream index, while `MRG32k3a` uses transition matrices ( $A$ ) which recursively evaluate ( $A^s \bmod m$ ) using the binary decomposition of  $s$ . The vector backend uses  $N$ (=SIMD length) consecutive substreams and also supports the scalar return-type which corresponds to the first lane of the vector return-type. Besides the `Uniform` method, some commonly used random probability distribution functions are also provided.

### 3.4 GeantV tracking and navigation

GeantV implements basketized vectorization of geometry navigation queries following the workflow described in section 2.1.2. Geometry “baskets” are passed to a top level navigation API, then dispatched to VecGeom to benefit from its vectorization features as described in 3.2.3. The geometry queries are integrated into the stepping procedure in a special `GeomQuery` stage, providing a large number of handlers, one per logical volume in the user geometry. Each query for computing the distance to the next boundary and safety within the current volume can be executed in either scalar or vector mode. The efficiency in the vectorized case depends very much on the volume shape and number of daughters. The track position and direction data are internally gathered into SOA data structures by VecGeom and dispatched the 3D-solid algorithms, updating navigation states held by the GeantV track structure. Note that even in the scalar calling sequence, VecGeom vectorizes the calls to the internal navigation optimizer.

An initial attempt to basketize and call the vector `DoIt` method for all volumes in a complex geometry

such as CMS proved to be inefficient. The main reason was not VecGeom vectorization inefficiency in multi-particle mode, but the impact of SIMD basketizing on the GeantV workflow. CMS geometry has  $O(4K)$  volumes, out of which  $\sim 80\%$  of the steps are performed in only  $\sim 10\%$  of the volumes. In a GeantV vector flow scenario, after an initial propagation out of the central vertex volumes, most tracks become isolated in SIMD baskets belonging to many different, less important volume handlers. The workflow enters starvation mode and has to force frequent flushes of these baskets and execution of geometry queries in scalar mode. The effect worsens for complex geometry setups, typical for collision events at LHC. In case of simple setups, composed of just a few geometry volumes, this scenario does not happen and basketization gains are evident in the case that the geometry code takes a sizeable fraction of the execution time.

To alleviate this effect, we implemented a new *dynamic basketizing* feature. Initially all volume basketizers are switched to ON, but the frequency of flushes versus vectorized executions is measured and triggers scalar mode for inefficient baskets. Depending on the tuned efficiency threshold, the prototype will end-up disabling most volume basketizers and keeping only about 5% active. Due to the fact that some shapes with intensive computation (such as polycone and polyhedra) are not vectorized in VecGeom in multi-particle mode, the overall vectorization efficiency is rather poor and offset by scatter/gather overheads.

Related to the geometry, GeantV uses a different strategy per step for the boundary crossing algorithm in magnetic field compared to Geant4. The algorithm first estimates the deviation of the particle moving with a given step along the helix arc in a small angle approximation, compared to a straight-line propagation with the same step. Constraining this bending error to be less than an acceptable tolerance gives the maximum allowed step in magnetic field,  $\delta_{\text{field}}$ . The geometry navigation interface is queried for the distance to the next boundary along a the straight line,  $\delta_{\text{boundary}}$ , as well as the isotropic safe distance within the current volume,  $\delta_{\text{safe}}$ . The propagation step is first constrained by the minimum between the physics step limit,  $\delta_{\text{physics}}$ , and the next boundary limit,  $\delta_{\text{boundary}}$ . The second constraint is the maximum between the magnetic field limitation and the safety. This allows particles with small momenta to ignore trajectory bending in the limit of nearby volumes, and particles with large momenta to ignore nearby volumes and travel forward much farther in the case that the deflection is small. In practice, this allows larger steps to be taken near volume boundaries without the risk of crossing accidentally. Finally, the step to be taken

is the minimum of either the geometry or the physics limit, within the field/safety constraint. This step is passed to the integrator algorithm to move the track to the new position. If it was the geometry that limited the step, the geometry is queried for a possible final relocation after the propagation, otherwise the algorithm is repeated until either the physics or geometry distance limits are reached. Note that after updating the track kinematics, tracks limited by geometry that have not completed crossing into the next volume are copied back into the geometry stage basket and considered in a subsequent execution of this stage, while the tracks having reached the next boundary are forwarded to the *PostPropagation* stage, as shown in Fig. 4.

### 3.5 EM Physics models and vectorization

The ultimate goal of the GeantV R&D activity is to exploit the possible computational benefits of applying vectorization techniques to HEP detector simulation codes. From the physics modelling point of view, the most intensively used and computationally demanding part of these simulations is the description of electromagnetic (EM) interactions of  $e^-$ ,  $e^+$ , and  $\gamma$  particles with matter. This is what motivated the choice of EM shower simulation code to demonstrate the possible computational benefits of applying track level vectorization.

Geant4 [24] provides a unique variety of EM physics models to describe particle interactions with matter, from the eV to PeV energy range, with different levels of physics accuracy. Each application area can find a suitable set of models with the appropriate balance between the accuracy of the physics description and the corresponding computational complexity. Moreover, Geant4 provides a pre-defined collection of EM physics models and processes for different application areas in the form of EM physics constructors [25]. Among these, the so-called EM *standard* physics constructor (i.e. EM Opt0) is recommended by the developers for HEP detector simulations.

A corresponding set of EM models have been provided for the GeantV transport engine, together with the appropriate physics simulation framework. The accuracy of each GeantV model implementation was carefully tested through individual model level tests by comparing the computed final states and integrated quantities (e.g. cross-sections, stopping power) to those produced by the corresponding Geant4 version of the given model. Moreover, several simulation applications have been developed to test and verify the GeantV EM shower simulation accuracy including both a general, simplified sampling calorimeter and a complete CMS detector setup. In all cases, the GeantV simulation results,

measured using quantities such as energy deposit distributions in a given part of the detector, number of charged and neutral particle steps, secondary particles, etc., agreed with the corresponding Geant4 simulation results to within 0.1% (see more in Section 4).

The final state generation, or interaction description, pieces of these models are the most computationally demanding subset of the physics simulation. At the same time, they provide the physics codes that can be the most suitable for track level vectorization. The final state generation usually includes the generation of stochastic variables, such as energy transfer, scattering or ejection angles from their probability distributions, determined by the corresponding energy or angle differential cross sections (DCS) of the underlying physics interaction. The probability density functions (PDF) are proportional to the DCS, which is usually a complex function and very often only available in numerical form. This implies that the analytical inversion of the corresponding cumulative distribution function (CDF) is unknown. For this reason, to generate samples of the stochastic variables needed to determine the final state of a primary particle that underwent a physics interaction, different numerical techniques have to be used.

The composition-rejection method, for example, is one of the most extensively used method in particle transport simulation codes to generate random samples according to a given PDF. However, it is not very suitable for vectorization, being based on an unpredictable number of loop executions depending on the outcome of the random variable. This implies that if this algorithm was vectorized over primary tracks, the different lanes of the vector would reach exit conditions in a non-deterministic way, at in different moments, thus reducing the number of used lanes, eventually causing a loss of any potential computational gain. For this reason, special care was taken to find new sampling algorithms, more suitable for vectorization, and also to implement solutions that could provide the maximum possible benefits of track level vectorization, even when applied to existing and well known sampling techniques.

As an outcome of this R&D phase, two solutions were implemented and tested in the GeantV EM Physics library. In GeantV jargon they are known as “sampling tables”, a solution that makes it possible to use an alias method in combination with sampling tables, thanks to the introduction of a discrete random variable as an intermediate step, and as “lane-refilling rejection” (hereafter rejection) to take advantage of vectorization even in the presence of non-deterministic sampling techniques. More details about the implementation of the

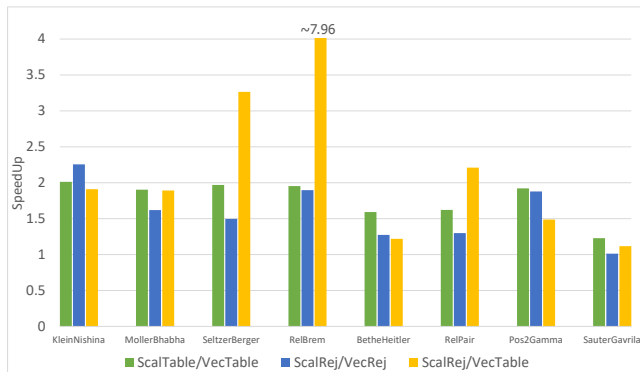


**Fig. 10** Speedup of the final state generation of different electromagnetic physics models obtained with SIMD vectorization in case of different sampling algorithms. The results were obtained by using Google Benchmarks [27] on an Intel® Haswell Core™ i7-6700HQ, 2.6 GHz, with Vc backend and AVX2 instruction set processing 256 tracks.

EM physics models and their vectorization can be found in Ref. [26].

Using the above mentioned model level tests to analyze the performance of the vectorized EM models over their (optimized) scalar versions, excellent  $\times 1.5$ -3 and  $\times 2$ -4 vectorization gains could be achieved on Haswell and Skylake architectures, respectively. The instruction set used on both architectures was AVX2, since AVX512 was not supported by Vc backend. Figure 10 shows the speedup of the final state generation of different electromagnetic physics models obtained with SIMD vectorization in the cases of the two different physics sampling algorithms.

As a result of these developments, the physics simulation part of the GeantV R&D activity provides the possibility of exploiting the benefits offered by applying track level vectorization on a complete EM shower simulation suitable for HEP detector simulation applications.

A relatively wide range of performance variation in the algorithms and their vectorization gain are observed. This is due to the fact that each of the EM physics models under study translates to a final state sampling algorithm with unique computational characteristics that is more favourable for one sampling technique or to the other. In addition to this it should be noted that while the sampling table based final state generations have a constant runtime under any external conditions, the efficiency of a given rejection algorithm can change significantly with the primary particle energy. This is illustrated in Fig. 11 that shows the relative speedup of these two techniques applied to the Bethe-Heitler  $e^-/e^+$  pair production model, as a function of the primary  $\gamma$  particle energy. The two algorithms perform similarly at lower energies while the rejection algorithm becomes

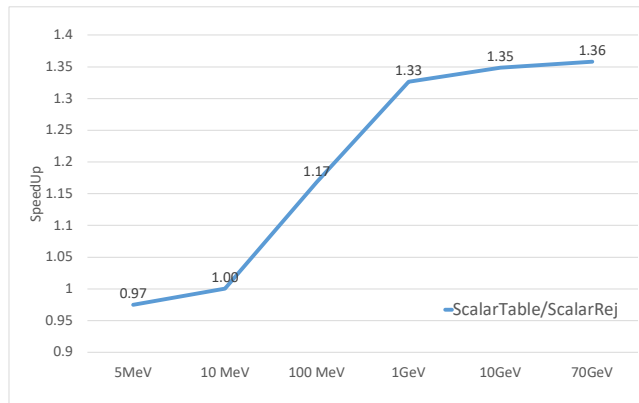


**Fig. 11** Speedup of the *rejection* based final state sampling compared to the sampling *table* based one in case of the Bethe-Heitler  $e^-/e^+$  pair production model.

$\sim 35\%$  faster at higher  $\gamma$  energies simply due to the smaller rejection rate.

The results shown indicate that the GeantV vectorized EM physics library has to be tuned to select the most efficient algorithm for any specific physics process, depending on the specific conditions. The complexity of the underlying DCS, the target material composition or the primary particle energy are examples of conditions that can heavily affect the physics performance. The GeantV physics framework has been designed taking all of these considerations into account, allowing the choice of the most efficient algorithm for final state generation, depending on the primary particle energy or detector region. This makes it possible to obtain maximum performance, while keeping the memory consumption of the algorithms under control, even in the case of the most complex HEP detector simulation applications.

### 3.6 Magnetic field integration

The integration of the equations of motion of a charged particle in a non-uniform pure magnetic field (or an electromagnetic field) accounts for about 15–20% of the CPU time of a typical HEP particle transport simulation.

The typical method for integration used is the family of Runge-Kutta methods, which involves the generation of multiple intermediate states  $(x, p)$ , the evaluation of the field and the corresponding equation of motion. Many floating point operations are carried out for each step of each track, providing substantial work for each initial data point, but without any expensive functions such as logarithms or trigonometric functions. In GeantV, the input to the field propagation stage is a basket of tracks. Each track has a requested step length for integration, obtained from the physical step size, the

distance to the nearest boundary and the curvature of the track (to avoid missing boundaries).

The tracks' positions are typically scattered throughout the detector. The integration of separate tracks is carried out in separate vector lanes in order to create the most portable code, and to make the best potential use of vector units with different widths.

The vectorization of this part of a particle transport simulation has some important characteristics: all steps of charged particles must be integrated, so long as the step can affect the deposition of energy or other quantities measured.

The lower level parts of the integration can be fully vectorized, because the operations proceed in lockstep, i.e. synchronously over the lanes of a vector with each lane corresponding to a different track:

- the evaluation of the EM field at each track's current or predicted location, either using interpolation (as in our benchmark example) or other methods such as the evaluation of a function;
- the evaluation of the 'force' part of the equation of motion using the Lorentz equation;
- and a single step of a Runge Kutta algorithm, which provides an estimate of the end state of a track (position, momentum) and the error of this end state.

The top-level of Runge-Kutta integration involves checking whether the estimated error conforms to the required accuracy, checking if a successful step finishes the required integration interval. If the integration goes on, it must also calculate the size of the next integration step.

Different actions are required depending on whether a step succeeded or not. In case a step was not successful or if the end of the integration interval was not reached, integration must continue for those tracks. A lane with a finished track, or one that reached the maximum allowed number of integration substeps, must be refilled from the potentially remaining pool of tracks in the basket.

Since all charged particles are involved, there is a large population of particles undertaking integration steps during a simulation. Larger-size baskets to accumulate work in field integration were created, and can be configured separately from the general basket size.

With larger baskets the fraction of lanes doing useful work increases substantially, getting close to unity, as shown in Table 3.

Unfortunately increasing the size of the buffer for field propagation has an additional effect, which counteracts the increase in efficiency from the reduction of idle lanes. It increases the number of simultaneous tracks in flight, as larger baskets accumulate more tracks. In turn this increases the memory usage, which is proportional

Basket size	Percentage of idle lanes	
	Default	Pre-processed
16	18.6	14.0
32	13.0	6.6
64	7.3	2.5
128	3.9	0.3
256	2.3	0.0
512	1.5	0.1
1024	0.7	0.1

**Table 3** Fraction of 'inactive' lanes, in which the integration has already finished, for different values of the basket size. Two configurations were measured: the default, in which tracks were processed in the original order of the basket, and the other ('pre-processed'), in which selected lanes with estimated work (length  $s$  over radius of curvature  $R$ ) over a threshold value were brought to the front of the basket. Measurements are from single-threaded simulations of 100 events, each with 10 primary electrons of 10 GeV energy in the CMS setup. The threshold used was  $s/R > 3$ .

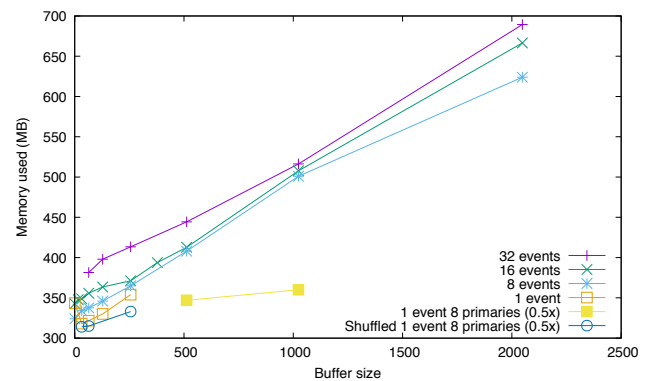


**Fig. 12** Memory size of a simulation versus the basket size for field propagation. Simulations with different number of simultaneous events are shown. The default number of primaries per-event is also varied, using 16 (default) and 8 primaries per event considered. All are single-threaded simulations of 100 events, each with 16 primary electrons of 10 GeV energy in the CMS setup. Run on MacBook Pro 2016 with 16GB RAM running MacOS 10.13.6.

to the the number of tracks in flight. The effects can be seen clearly in Figure 12, where a linear relation between the buffer size for field propagation and the memory use is evident. It is possible however to reduce memory use by starting fewer simultaneous events, as seen in the additional measurements with 1, 8, 16 or 32 simultaneous events.

### 3.7 Input and output (I/O)

#### 3.7.1 Input

Simulation input consists of particles to be transported through the detector. These can be either realistic collision events produced by Monte Carlo event generators or single-particles (like a test beam) to study a particu-

lar response. The use of an interface (the so-called *event record*) makes the generation and the simulation steps independent, as schematically shown in Figure 13. For the GeantV transport engines it is irrelevant how the ‘primary’ (input particles) are produced. The simulation threads concurrently process particles from the input.

The interface to the HepMC3 [28] event record has been implemented (the `HepMCGenerators` class). This interface can read both HepMC3 ASCII as well as ROOT files. The different types of input files are recognized by the extension. The interface selects the stable (outgoing) particles from the provided event and passes them to the transport engine. It can also apply optional cuts, for instance on  $\eta$  (pseudorapidity),  $\phi$  (azimuthal angle), or momentum.

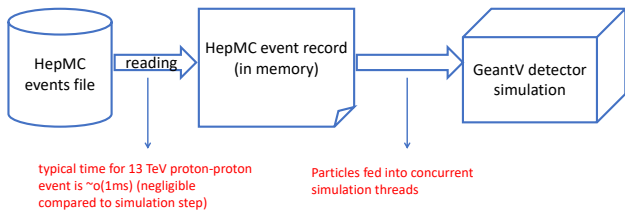


**Fig. 13** HepMC event record used as GeantV input format.

### 3.7.2 Output

The detector simulation produces *hits*, i.e., energy deposition and timing information in the sensitive parts of the detector, which are the output of the program. In the case of GeantV, those hits are produced concurrently by all the simulation threads and need to be recorded properly. Thread-safe queues have been implemented to handle the asynchronous generation of hits from several threads simultaneously. The GeantFactory machinery takes care of grouping the hits into so-called HitBlocks and putting them in the queues. Two possible approaches were tried for saving the hits into a file. In the first, all the hits produced by different threads were given to one ‘output thread’ for serialization. This approach turned out not to scale properly and was appearing as a bottle-neck. The problem was solved by the second approach, where the serialization was performed by each transport thread and the ‘output thread’ was only responsible for the actual writing of the data to the file. This approach did not adversely affect the memory consumption in any visible way. The implementation is based on the TBufferMerger class provided by ROOT [29]. Each transport thread fills, in parallel, its ROOT TTree objects, and the TBufferMerger merges these TTrees and saves them into the physical file, as shown in Fig. 14.

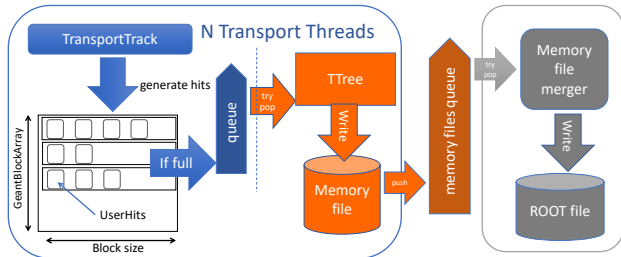


**Fig. 14** Output architecture based on ROOT’s TBufferMerger.

This architecture has been benchmarked and shows very good scaling behaviour, Figure 15. In particular it solves the bottleneck problem of the ‘single thread serialization’ approach.

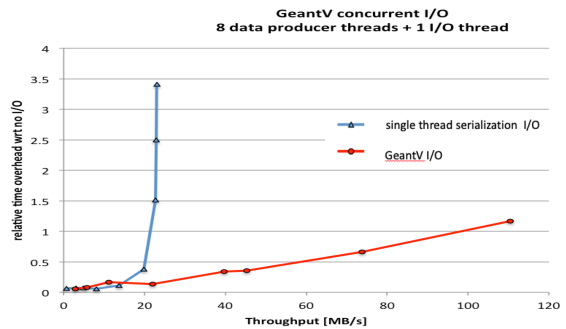


**Fig. 15** I/O performance compared to ‘single thread serialization’. Intel(R) Xeon(R) CPU E5-2630 v3 @ 2.40GHz (Haswell), 2x8 cores, HT=2 (i.e. 16 native threads, 32 in hyperthreading mode), disk: SSD 430 MB/s non-cached write speed (measured with: `dd if=/dev/zero of=/tmp/testfile bs=1G count=1 oflag=direct`).

### 3.7.3 MC truth

In addition to the hits users may be interested in saving the kinematic output, so-called *MC truth* information, i.e., the particles (or at least some of them) that produced those hits. The handling of MC truth is quite detector dependent and no general solution exists. The algorithms selecting which particles to store, how to keep connections between them, and how to associate hits to them are not straightforward and, most of the time, require some trade-offs between the completeness of the stored event information and its size. In general, we do not want to store all the particles, as this would only waste the disk space without providing any useful information. For instance, we typically do not want to

store delta-electrons, low-energy gamma showers, etc. We want to store all the particles needed to understand the given event and to associate hits to them. In all cases, we need to make sure that the particles connections are set in a way to form consistent event trees.

In addition to all the above, multi-threading and concurrency only increases the complexity, because the order of processing the particles is non-deterministic. There are situations where, depending on the load of the processor, processing of the ‘daughter’ particle may be completed before the ‘mother’ particle’s ‘end of life’. Then events need to be reassembled from the products generated by the different threads after parallel processing.

Following the idea that no MC truth-handling strategy is perfect, nor complete, we need to give users a way to decide which particles to store. The GeantV particle transport needed, therefore, to provide the possibility of flagging particles as ‘to be stored’ according to some user defined rules and, at the same time, to ensure that the stored event has consistent mother-daughter links, as well the correct hit associations. Taking all these requirements into account, MC truth handling was implemented using an architecture that has a light coupling to the transport engine, providing minimal ‘disturbance’ to the transport threads and at the same time providing the flexibility to implement custom particle history handlers. In this design, shown in Fig. 16, the interface provided by the MC truth manager (MCTruthMgr class) receives (concurrent) notifications from transport threads about adding new primary or secondary particles, ending particles, or finishing events. It then delegates the processing of particles’ history to a concrete MC truth implementation. In other words, the implementation is composed of the MCTruthMgr class providing the interface and the underlying infrastructure for the particles’ history (with a light-weight, transient, intermediate event record) and the user code that implements the decision making (filtering) algorithm, as well as the conversion to the users’ event format. As a proof of principle, we have provided an example using HepMC3 as the MC truth output format. We have demonstrated how to implement a simple filtering algorithm based on particles’ energy, allowing a consistent particle history to be serialised into an output file.

### 3.8 User interface

GeantV provides ‘user actions’ (similar to those in the Geant4 toolkit) allowing to control the program flow at the level of run, event, track and step. Concurrent containers allow users to accumulate different kinds of information and merge the information from the

different threads at the end of the run. Scoring is done using dedicated stepping actions where the sensitive volumes are checked.

#### 3.8.1 Scoring interfaces

The GeantV prototype implemented specific scoring interfaces aimed at facilitating handling user-defined data structures for mixed concurrent events. The concurrency aspect is handled by having multiple copies of scoring data structures attached to GeantV task data objects. Each running worker thread picks up a different task data object, percolating it as an argument to the user scoring interfaces. Since the maximum number of events transported concurrently,  $N_{\max}$ , is limited, the user scoring data structures have to be indexed in arrays having the same limit:  $N_{\max}$ . The user type has to be trivially default constructible and copiable, and has to implement methods to merge and clear the data for a given event slot. The users are provided the interface to attach custom data types to each task, usable subsequently in their application for scoring in a thread safe way. A detailed example using this pattern can be seen in the CMSFullApp example from the GeantV Git [30] repository.

## 4 GeantV applications and physics validations

The complexity of detector simulation software requires rigorous testing and continuous monitoring during development in order to ensure code correctness and to keep simulation precision and computing performance under control. Several tests and applications, with different levels of complexity, have been developed in order to meet these needs.

Particle transport simulation is composed of several individual components, including the geometry modeler, material description, physics models and processes, held together by the simulation framework. The framework is used to setup a flexible modelling environment, including a generic computation workflow controlled by upper level manager objects. As a consequence, the individual building blocks are accessed through their interfaces and provide their functionalities through the framework. Checking the correctness of individual components is a pre-requisite for ensuring the above-mentioned quality criteria. Then, using complete simulation applications that exploit and exercise the whole simulation framework is an essential final step in this testing procedure.

Model level tests allow the verification of the responses of individual physics models by directly calling their interface methods. This makes it possible to test in

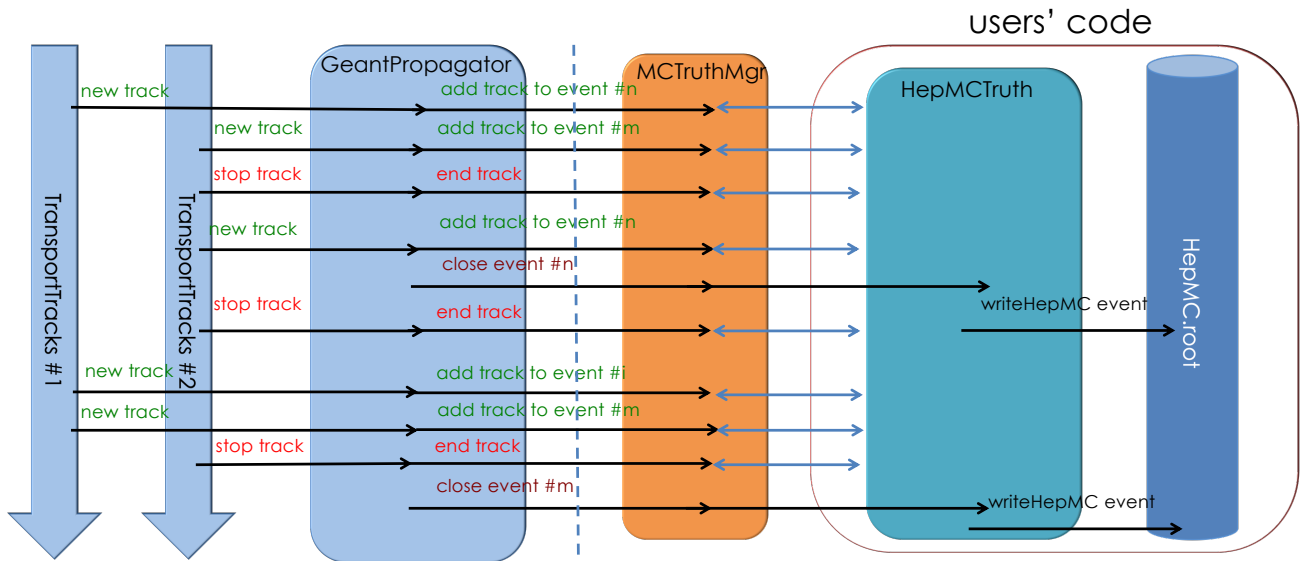


**Fig. 16** Example MCTruth-handling architecture based on the GeantV MCTruthMgr class and HepMC event record as user's output format.

an isolated way the correctness of the integrated quantities (e.g. atomic cross section, stopping power, etc.) and differential quantities (e.g. energy/angular distribution of the final state particles) that the physics models provide during the simulation. We enforced producing such model-level tests as part of the physics model development procedure. The results were verified by comparing with theoretical expectations and to the corresponding Geant4 tests.

To test and validate the overall simulation framework, including its building blocks, complete simulation applications were developed, together with the corresponding Geant4 applications, if these were not already available.

An application with a simple setup (**TestEm5**<sup>1</sup>), with a configurable particle gun and a configurable target, was developed as a first-level test application. In spite of its relative simplicity, this application can produce several integrated quantities (e.g. mean energy deposit, track length, number of steps, backscattering and transmission coefficients, etc.) and differential quantities (e.g. transmitted/backscattered particle angular/energy distributions). The primary particle and target properties can be modified easily. This application was then the per-

fect tool for primary testing, validation and debugging during the development of the physics framework.

The second application developed was a generic, simplified sampling calorimeter simulation (**TestEm3**), similar to that used for monthly validation by the Geant4 electromagnetic (EM) physics developers. With its intermediate complexity, this application was used for verification of the simulation by comparing several differential and integrated quantities to those provided by the corresponding Geant4 simulation. As an example of such a differential quantity, the mean energy deposit by  $E_0=10$  [GeV] electrons as a function of the layer number (proportional to the depth) is shown in Fig 17 and compared to the corresponding Geant4 (version 10.4.patch03) simulation results. Integrated results, such as the mean energy deposit, track lengths in the absorber and gap materials or the mean number of secondary particles and simulation steps obtained from the same simulation setup, are summarised in Table 4. Note, that all the quantities are within per mil level of agreement compared to the corresponding values obtained by using Geant4.

Finally, a simulation application using the complete CMS detector (**FullCMS**) was developed in order to validate and verify the correctness and robustness of the overall framework when reaching the complexity of an LHC experiment. While a similar level of agreement

<sup>1</sup> whenever they existed, names were matched to the corresponding Geant4 application

as mentioned above was found between the GeantV and the corresponding Geant4 simulation results, these applications were mainly used for performance analysis and profiling.

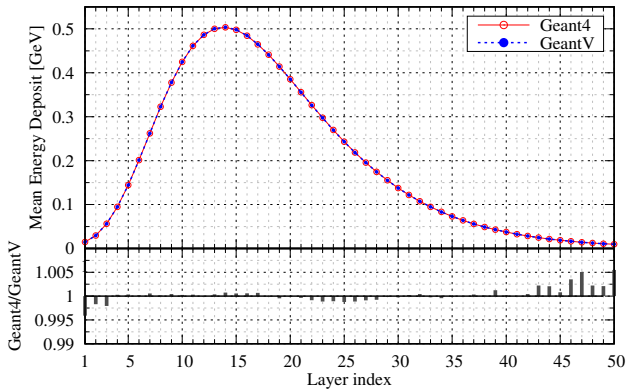


**Fig. 17** Mean energy deposit by  $E_0=10$  [GeV]  $e^-$  in a simplified sampling calorimeter as a function of the layer number simulated by GeantV and Geant4 (10.4.patch03). The calorimeter is 50 layers of 2.3 [mm] lead and 5.7 [mm] liquid argon. A 4 [T] transverse magnetic field was applied and 0.7 [mm] secondary production threshold was used.

## 5 Usability aspects

### 5.1 Reproducibility

Due to the stochastic nature of particle physics processes, detector simulation results are influenced by the generated random number sequence. Different sequences will generally produce slightly different, but statistically compatible, results. Such sequences are pseudo-random, being controlled and reproducible based on an initial ‘seed’ (the next generated number is fully determined by the current generator state). Reproducibility is an important requirement in the case of HEP detector simulation: simulations with the same initial configuration (primary particles and pRNG choice and seed) must give the same results. Even in case of non-sequential processing, the simulation must be repeatable when starting from the same initial configuration of the pseudo-random number generator (pRNG) engine. This must hold true even if different choices are made during a run, e.g. using vector kernels for a set of physics processes of selected tracks. A key practical reason is the need to reproduce and debug problems that occur during the simulation of a particular event or initial particle. Besides, the reliability of a simulation that cannot be exactly repeated is more difficult to assess.

In GeantV, baskets of tracks undergoing the same interaction are accumulated to enable computations based on vectors of track properties, aiming to use these vectors for the bulk of the computational work. The remaining tail of tracks is treated with sequential (non-vectorized) code, but using the same algorithms as the vector code. Multi-threading is used to gather larger populations of tracks having similar properties and enable wider vectors, targeting more efficient use of the vector code and higher performance. Due to the out-of-order execution in multi-threading, the track content of baskets is not preserved in each run. In addition, a different set of remaining ‘unbasketised’ tracks is run in scalar mode in each run, in particular during the ramping down phase of the simulation. To be reproducible, a particular algorithm must obtain the same pRNG output value (variate) for a track, whether it is processed as part of a vector in a basket of tracks (‘vector’ mode) or as a single track using the non-vectorized code (‘scalar’ mode).

To obtain the same results for a track’s physics interactions (or other operations), the same sequence of output values of a pRNG is needed. This is achieved by associating a single pRNG state with each track. Whenever a new track is created, either as a primary particle or in a process, a deterministically-defined new state of the pRNG must be generated and associated with it. This idea, called ‘pseudo-random’ trees, was first proposed in the 1980s in a particle transport application [31]. A first implementation was also created using linear congruential generators. Applications in other parallel and branching computations have been proposed since – the recent review of Schaathun [32] has an overview and an evaluation of the proposed methods. One such method for constructing seeds, called the *pedigree* method, was developed for constructing seeds was developed by Leiserson et al. [33] exploiting deterministic parallel computations written in Cilk. This method was implemented in particle transport simulation [?] using Geant4 [24] as a testbed.

How such splittable/tree pRNGs can be used in practice has been demonstrated, within the constraints of a particle transport program which mixes vector and scalar code and which can be run in either single or multi-threaded modes. The overhead of our implementation was measured, compared to simulations that do not use these methods, and, as a result, do not reproduce the same results between runs. Several considerations and key aspects of the implementation are discussed.

The approach adopted for GeantV depends on two pieces: first, an initial seed for the scalar mode or a set of seeds for the vector mode is assigned; second, a unique sub-stream index is determined for each track.

$3 \times 10^5 E_0=10$  [GeV]  $e^-$  in simplified sampling calorimeter: 50 layers of [2.3 mm Pb + 5.7 mm LAr]; cut = 0.7 [mm]

e <sup>-</sup> , e <sup>+</sup> and $\gamma$ interactions; 4 [T] magnetic field								
Geant4					GeantV			
material	E <sub>d</sub> [GeV]	rms* [MeV]	tr.l. [m]	rms [cm]	E <sub>d</sub> [GeV]	rms* [MeV]	tr.l. [m]	rms [cm]
Pb	7.6220	68.787	5.4071	5.0523	7.6383	68.857	5.4187	5.0566
LAr	2.2367	53.0346	11.1017	27.2538	2.2207	52.5708	11.0255	27.0225

Mean number of :

gamma	5181	5179
electron	8891	8899
positron	534.5	534.5
charged steps**	36572	35887
neutral steps	35030	35063

**Table 4** Detailed results of the simulation from irradiating a simplified sampling calorimeter with electrons: mean energy deposit ( $E_d$ ), charged particle track length (tr.l), mean number of secondary  $e^-$ ,  $e^+$  and  $\gamma$  as well as the mean number of steps made by charged and neutral particles. Notes: \* more statistics required to see the agreement between the RMS values; \*\*geometry is always called before the physics step limit (i.e. at the pre-step point) in case of GeantV that results slightly different step-limit in case of  $e^-/e^+$ .

The stream index for the primary track consists of high precision bits set by the event number and low precision bits by the track index. For the secondary (or daughter) tracks, the stream index is generated in a collision-resistant way using the current state of the pRNG carried by the (mother) track that undergoes an interaction.

To enable reproducibility of the vector code for physics processes, a vector pRNG must be created in order to generate the output in each vector lane of the pRNG corresponding to each track index in the basket. In our design this role is played by an instance of a proxy class, acting as a vector pRNG. The proxy provides all the expected outputs in each vector lane (as individual pRNG's would behave for each track) and advances the state of each track's pRNG accordingly. The first implementation of a proxy class gathered the contents of the scalar pRNGs into an instance of the corresponding VecRng class (e.g. gathering MRG32k3a<double> into MRG32k3a<Double\_v>). The proxy instance is reusable, by explicitly attaching and detaching the set of track pRNG states.

Reproducibility was tested using a limited set of GeantV physics processes, including bremsstrahlung, ionisation, and Compton scattering, which undergo a self-contained  $e^- - \gamma$  cascade process. The pRNG used in the tests is ThreeFry from the Random123 package [19]. This counter based generator was chosen because the stream is easily split in separate sequences, the state size is moderate (128 bits), and the method of initialization from a seed is trivial.

The number of tracks and steps of a simulation of 1000 events, each comprised of ten 10 GeV electrons impinging on a 50 layer lead and liquid argon calorimeter, was compared. The number of tracks and steps of scalar and vector configurations, with either 1 or 4 threads

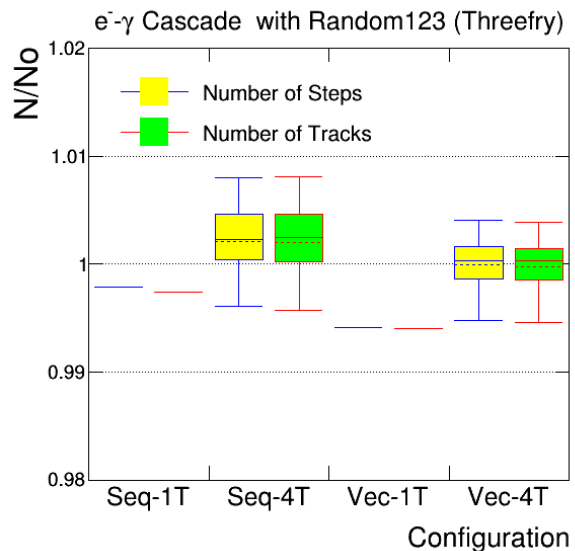


**Fig. 18** The ratio of the total number of tracks (steps) of the default (non-reproducible) mode normalized to the reproducible configuration of which the total number of tracks (steps) is  $N_0$ . 10 GeV  $e^-$  tracks are tested with scalar (Seq) and vector (Vec) configurations with 1-thread (1T) and 4-threads (4T).

each has been compared. The simulation was run in two modes: the default mode, in which a per-thread state of one serial pRNG and one vector pRNG are used in each thread; and the 'reproducible' mode in which the method described above is used. Using the values for the 'reproducible' mode run with 1 thread as a baseline (Seq-1T), the ratios of the number of tracks and steps are shown in Fig. 18.

It is verified that the reproducible mode maintains the constant number of tracks and steps for all tested configurations, as required. In addition, those numbers are different from the single threaded mode for each

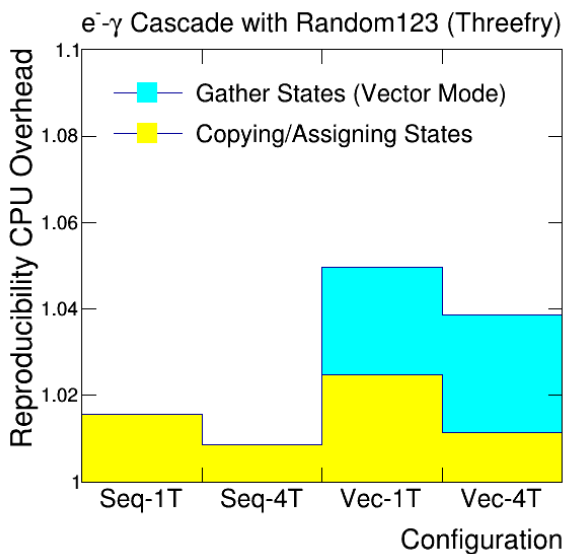


**Fig. 19** The overhead of the reproducibility in simulation (CPU) time for the strategy using gathering scalar states to a vector state for different configurations and splitting states vice versa. 10 GeV  $e^-$  tracks are tested with scalar (Seq) and vector (Vec) configurations with 1-thread (1T) and 4-threads (4T).

of the 1-thread (Seq-1T) and vector 1-thread (Vec-1T) modes by 0.2 – 0.6%. In multi-threaded mode, the number of tracks and steps fluctuates as expected, with averages (and variances) within one sigma of the values of the reproducible mode.

Reproducibility introduces an overhead in the simulation due to copying and assigning pRNG states during the simulation workflow, gathering scalar states to a SIMD vector state or joining-splitting states for the proxy approach, and synchronizing the index of states in output (Random123 specific). Figure 19 shows an example of the CPU overhead as the fraction of  $\text{Time(Reproducibility)}/\text{Time(Default Mode)}$  using gathering scalar pRNG states to a vector state and splitting states vice versa. Another approach using the join-split method shows a similar (2-5%) performance degradation for the reproducibility mode.

Alternative proxy implementations are under development, including one that avoids the cost of copying the data. This is of most interest for the cases in which the average number of variates required is small and/or the pRNG state is large.

## 5.2 Experiment framework integration

The Compact Muon Solenoid (CMS) experiment uses a custom, fully-featured, multithreaded software framework called CMSSW [9, 35, 36, 37]. This software frame-

work is used to produce billions of simulated events every year, employing the Geant4 simulation toolkit. In addition, CMSSW handles various other components including event generation, detector geometry, magnetic field, and scoring. The last component includes the creation of simulated hits that are used as input for custom electronics simulations.

The most important test of GeantV with CMSSW was to demonstrate the compatibility of the threading models. In production, CMSSW uses event-level parallelism with Geant4. This approach isolates each event in its thread. By avoiding communications between threads, the thread-safety of the application is easier to guarantee. In contrast, GeantV may process tracks from multiple events together in multiple threads. The GeantV approach was first tested in a simplified multithreaded framework that uses the same Intel® Thread Building Blocks (TBB) [38] task-based processing as CMSSW. This test was successful and led to the development of an external loop mode for GeantV, in order to allow the experiment’s software framework to control the distribution of tasks to threads.

Subsequently, the GeantV engine was fully integrated into CMSSW. To allow a more efficient trading of tasks between CMSSW and GeantV, a new CMSSW framework feature called ExternalWork is employed [39]. With ExternalWork, the actions of the CMSSW module that runs GeantV are split into two steps, acquire and produce. In the acquire step, the input event data is obtained and sent to GeantV. The acquire step is non-blocking, so it returns control of the thread after spawning a task for GeantV to process the event. Once GeantV has finished processing the event, it executes a callback function, which adds the produce step to the TBB task queue. In the produce step, the CMSSW output products are created and placed in memory. This is depicted in Fig. 20. Without the use of asynchronous callbacks, the framework could be blocked if an event is loaded in one thread but then finishes processing in a different thread, after GeantV basketizes the event’s tracks together with other events. In the future, it may be possible to decouple the loading of event data from the spawning of tasks by making the external loop mode more sophisticated, which could further increase the efficiency of this kind of parallel processing.

To demonstrate the full compatibility of GeantV with the experiment software framework and the steps necessary to reuse Geant4-based applications with the new transport engine, all of the additional components mentioned above are important. It is straightforward to convert generated events, stored in the HepMC format [40], into native GeantV input. The CMS detector geometry can be converted into a TGeo [29] represen-

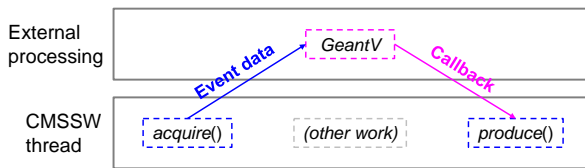


**Fig. 20** The ExternalWork feature in CMSSW, showing the communication between the experiment software framework and GeantV.

tation, which is automatically recognized by GeantV and can be navigated by VecGeom. For simplicity, a constant magnetic field of 3.8T is used.

The scoring code required significantly more effort to adapt. There are two approaches to scoring in Geant4: sensitive detectors or watchers. Sensitive detectors are classes assigned to sensitive volumes, whose methods are automatically called when tracks traverse those volumes. This approach is the most efficient, because the volume name does not have to be checked. In contrast, watchers check every volume before deciding if they should execute their methods and record hit data. The second approach was chosen for the compatibility demonstration because the first approach is not available in GeantV and, in addition, as currently implemented in CMSSW, the first approach has more dependencies on Geant4 classes.

The full suite of scoring classes for the CMS detector comprises roughly 10,000 lines of code. A simplified scoring class that handles the electromagnetic and hadronic calorimeters (ECAL and HCAL) was used as a demonstrator. These detectors were chosen because their scoring algorithms are relatively complex, relying on many Geant4 objects and interfaces, and because they are sensitive to the electromagnetic physics processes that have been vectorized in GeantV. The goal was to be able to use the exact same scoring code with both Geant4 and GeantV, to avoid regressions or increased maintenance burdens. Both the objects and interfaces differ between Geant4 and GeantV, so the demonstrator class is turned into a class template, where the template parameter is a traits class that collects all relevant objects and aliases them to common names. To address the differences in interfaces, specialized wrapper classes, with consistent methods, are provided for both Geant4 and GeantV. These wrapper classes handle the event, step, and geometry volume objects. This approach, using template wrappers and traits classes, has several benefits. It allows complete reuse of the scoring code with virtually no changes in the implementation, and it has no impact on performance, because the templates are evaluated at compile time.

However, there is another element to scoring in GeantV: thread-safety. In Geant4, as mentioned, each event is isolated in its thread, so having one instance of each scoring class per thread suffices. In GeantV, because tracks from multiple events are processed in multiple threads, steps for a given event may occur in different threads simultaneously. Rather than upsetting the complex scoring code by trying to make the existing classes accept input from multiple threads without causing data races, we took the approach of having one instance of the scoring class per thread, per event. When a given event finishes processing in GeantV, the per-thread scoring classes dedicated to that event merge their output into a cache associated with the event, which is also accessible to CMSSW. This aggregation process is supported by the `TaskData` construct in GeantV, as depicted in Fig. 21. The duplication of scoring class instances can increase the memory usage; however, this is mitigated by sharing read-only members, such as maps of detector volumes, between instances of the class.

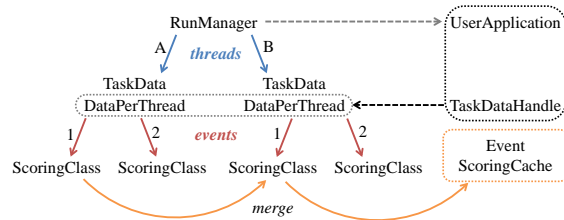


**Fig. 21** The process of aggregating scoring information from events being processed in multiple threads.

With all of these elements in place, equivalent simulations can be run in CMSSW using Geant4 and GeantV. This allows testing of both physics and computing performance, which are reported in Sect. 6.6. The CMSSW module and supporting code that demonstrates the integration of GeantV can be found at Ref. [41].

## 6 Performance results

In this section, an investigation of various performance aspects of the GeantV prototype is presented. Both a simplified example of a sampling calorimeter and a complex application that uses the CMS geometry and complete EM physics were used as benchmarks.

Several configurations of the core GeantV engine were tested to highlight the contribution of different components to the observed overall performance. Two key aspects of performance were examined: the intrinsic performance of the GeantV applications by looking at various performance counters, and comparisons between

different configurations of both GeantV applications with the equivalent applications running in Geant4. Finally, the performance from the user’s perspective, by modifying the CMS simulation application to accommodate the GeantV engine with scoring, and comparing with the existing similarly configured Geant4-based application was examined as well.

Simulation performance has multiple dependencies on different parameters. The most important is the complexity of the application itself. Changing production cuts, tracking cuts or tracking precision can result in orders of magnitude differences in the number of simulated particles and steps. The benefits of running an application in the GeantV framework can vary hugely when different cuts are applied. The geometry complexity and the magnetic field setup are other application-dependent parameters that can greatly affect the CPU profile.

Another dimension to explore is the performance dependence on the hardware architecture (CPU, vector architecture, cache layout), and on the compiler and optimization flags. Measurements on several different systems were performed, although the current coverage is far from being complete. This analysis gives insight into how the application manages scarcity or abundance of various resources and consequently highlights areas where performance is good as well as areas to improve.

Finally, different configurations of GeantV were explored, varying basket size and the size of the event cache, switching basketization on/off and emulating single track transport. This provides insight into the performance of individual components or scheduling features.

## 6.1 Global performance

A set of global performance metrics for the GeantV examples to be compared with the equivalent Geant4 ones were selected: total execution wall clock time, instructions per cycle (IPC) and FLOPS per cycle (FPC), computational intensity (FLOPS per memory operation - FMO), and the fraction of vector instructions (single and double precision). Cache misses at different levels, as well as TLB (translation lookaside buffer) misses were also evaluated. These global counters using default GeantV settings by varying only the complexity of the application were examined. We also tested on different platforms with different vector architectures and CPU cache configurations.

For the performance benchmark results and comparisons described in this section, equivalent standalone CMS applications of GeantV and Geant4 were used (unless otherwise stated). These utilised the 2018 CMS

GDML detector description and a magnetic field map interpolating a grid of field values extracted from CMSSW. The default scheduling mode used for GeantV is an optimized vectorization mode in which basketization and vectorization are turned on for all sub-modules except for geometry; other modes will be specifically mentioned whenever appropriate. The 8.3.0 version of GCC was used with the default optimization level (`-O3`) and build type (`Release`). An input of 1000 events of sixteen 10 GeV electrons was simulated on dedicated quiet machines where the measurement uncertainty was less than 0.5%.

Table 5 and Table 6 show characteristics of several hardware platforms tested for performance comparisons and results of CPU benchmark of GeantV (version beta) compared to Geant4 (version 10.5) using the CMS detector, respectively. The hardware platforms considered are Intel E2620 (Sandy Bridge), Intel E2680 (Broadwell), and AMD 6128 (Opteron). As shown in the column, “Speedup” in Table 6, the relative performance ratio of Geant4/GeantV in CPU widely varies on different platforms. The impact of different configurations of the magnetic field on the relative speedup is marginal on the same hardware platform shown in Table 7, as an example, on Intel E2620.

**Table 5** Hardware platforms used for performance tests: CPU [GHz], Memory [GB] and L3 Cache size [MB].

Processor	CPU	Memory	L3 Cache
Intel E2620 (Sandy Br.)	2.0	32	15
Intel E2680 (Broadwell)	2.4	128	35
AMD 6128 (Opteron)	2.3	64	12

**Table 6** Performance comparison between GeantV and Geant4: The average CPU time in seconds per event for simulating  $16 \times 10$  GeV electrons propagating through the CMS detector and the magnetic field.

Processor	SIMD	Geant4	GeantV	Speedup
Intel E2620	AVX	4.94	2.33	2.12
Intel E2680	AVX2	2.18	1.63	1.43
AMD 6128	SSE4	6.63	4.33	1.53

It turns out that Geant4 performance is more sensitive to the size of cache memory and fluctuates more widely compared to GeantV. An extended performance benchmark study on various hardware platforms and different compilers is also available in Appendix B.

**Table 7** Performance comparison between GeantV and Geant4: The impact of different configurations of the magnetic field on Intel E2620 (Sandy Bridge). Ratios of G4/GV and G4/GV(vect) are relative gain of GeantV with respect to Geant4 using the scalar mode and the vector mode of GeantV, respectively.

Configuration	GeantV [s]	G4/GV	G4/GV(vect)
Zero-field	1794	1.86	1.95
Uniform (3.8T)	2412	1.97	2.19
CMS field map	2621	1.88	2.12

There are a variety of performance metrics (hardware counters) provided by PAPI (performance application programming interface) [42]. A combination of PAPI counters provides useful information of code performance, such as floating-point operations, instruction per cycle, cache behaviours, memory access patterns and so on. For example, floating-point operations per cycle is a good measure for the CPU utilization while instruction per cycle (IPC) quantifies good balance with minimal stall. For collecting profiling information along with hardware counters, we use OpenSpeedshop [43] as the primary profiler, which provides an integrated toolkit and analysis framework for various performance experiments and measurements. Table 8 shows IPC of GeantV compared to that of Geant4, which indicates that GeantV executes relatively more instructions per cycle. Since instructions completed is approximately proportional to the total floating-point operations, FLOPS/Cycle of GeantV with respect to Geant4 also follows the same pattern as IPC.

**Table 8** Instruction (INS) per cycle (CYC), IPC of GeantV compared to Geant4.

Processor	GeantV		Geant4	
	INS/CYC	IPC	INS/CYC	IPC
Intel E2620	7038/6610	1.06	8388/10788	0.78
Intel E2680	6474/5521	1.17	8914/5514	1.62
AMD 6128	7813/8839	0.88	8459/11228	0.75

Another important performance metric is floating point operations per memory operation (FMO), which quantifies data locality or computational intensity. Table 9 shows FMO of GeantV compared to that of Geant4, which implies that GeantV has better data locality than Geant4 in these tested platforms even though they widely vary due to the different cache sizes and policies. Nevertheless, FMO is relatively small for both Geant4

and GeantV, which indicates that the typical HEP detector simulation is a memory-bounded application.

**Table 9** Floating-point instructions per memory operation (FMO) in terms of floating point operations (FO) over the sum of load instructions (LD) and store instructions (SR).

Processor	GeantV	Geant4
	FLOP/(LD+SR)	FLOP/(LD+SR)
Intel E2620	1718/3402 (0.50)	2181/5509 (0.40)
Intel E2680	2347/1758 (1.34)	3824/3100 (1.23)
AMD 6128	3191/3704 (0.86)	1620/5515 (0.29)

Nonetheless, the resultant speedup and the platform dependency are not driven by a set of functions or libraries. For example, the percentage of the total CPU time by Geant4 library, shown in Table 10, is very comparable on different hardware platforms. This is also true for GeantV as shown in Table 11, which indicates that the relative speedup seems to be a global effect spread over all the code.

**Table 10** Percentage CPU time spent in each Geant4 library for simulating  $16 \times 10$  GeV electrons propagating the CMS detector.

Library (%)	Intel	Intel	AMD
	E2620	E2680	6128
libG4geometry.so	41.8	43.6	42.3
libG4processes.so	22.0	20.8	21.0
libG4global.so	7.3	8.0	7.5
libG4tracking.so	7.3	6.5	7.2
libG4track.so	6.0	4.7	5.8
full.cms	5.2	6.1	6.6
libG4clhep.so	3.3	3.0	3.0
libm-2.12.so	2.7	3.5	2.9
libG4particles.so	1.2	0.7	1.0
libG4digits_hits.so	1.1	1.3	1.0

To understand the underlying cause of the overall performance difference between Geant4 and GeantV, instruction and data cache misses at different levels were also studied. Table 12 and Table 13 show instruction and data cache misses in L1 and L2. In both cases, the GeantV application shows far fewer instruction cache misses, which is attributed to the fact that GeantV has much simpler code structure and consists of smaller libraries.

Most modern hardware systems have a TLB (translation lookaside buffer) which serves as the cache for page tables that map addresses between virtual memory and physical memory. Table 14 show both instruction

**Table 11** Percentage CPU time spent in each GeantV library for simulating  $16 \times 10$  GeV electrons propagating the CMS detector.

GeantV Library (%)	Intel		AMD
	E2620	E2680	6128
libGeant_v.so	42.1	46.3	43.2
libRealPhysics.so	36.0	34.2	37.3
libGeantExamplesRP.so	14.1	14.1	14.5
libc-2.12.so	3.8	1.8	1.1
libVmagfield.so	3.1	2.8	3.1
libm-2.12.so	0.6	0.6	0.6

**Table 12** L1 cache misses in 1 Billion hardware counters between Geant4(G4) and GeantV(GV): ICM and DCM are Instruction and Data Cache Misses, respectively. The Level 1 latency is typically 3 cycles.

Processor	ICM		DCM	
	GV	G4	GV	G4
Intel E2620	54	429	218	269
Intel E2680	39	511	188	272
AMD 6128	49	309	141	144

**Table 13** L2 cache misses in 1 Billion hardware counters between Geant4(G4) and GeantV(GV): ICM and DCM represent instruction and data cache misses, respectively. The Level 2 latency is typically 12 cycles.

Processor	ICM		DCM	
	GV	G4	GV	G4
Intel E2620	19	36	86	46
Intel E2680	23	29	101	51
AMD 6128	17	3.6	55	10

and data TLB cache misses of GeantV compared to those of Geant4. Note that there are drastic differences in instruction TLB misses on Intel E2620 and data TLB misses on AMD 6128. However, it turns out that the total cost for TLB misses is a relatively small fraction of the total elapsed time - For example, the 330 million TLB misses on the Intel E2620 cost about one second.

## 6.2 Scheduler performance

Tried to quantify the impact of different parameters: number of events in flight, basket size, scalar emulated mode against basketized mode, the performance of the GeantV workload scheduler was evaluated. The observed vectorization gains per component were measured. The performance impact of the cool-down phase when basketization is less efficient was also evaluated. The GeantV

**Table 14** TLB misses in 1 million hardware counters between Geant4 (G4) and GeantV (GV): IM and DM represent instruction and data TLB misses, respectively. The TLB miss latency is typically 6 cycles.

Processor	IM		DM	
	GV	G4	GV	G4
Intel E2620	53	4256	3168	4626
Intel E2680	N/A	N/A	24	82
AMD 6128	55	149	88	1628

scheduler has an option to run in single track mode which emulates Geant4-style sequential tracking. Table 15 shows the performance of GeantV single track mode compared to the default (basketized) mode, which shows marginal variations on different platforms. Therefore, the impact of the GeantV scheduler or data locality is not the primary source of performance difference between Geant4 and GeantV in scalar mode. Note that computing performance depends on the basket size for the magnetic field, for physics, and for the multiple scattering process and may need to be optimized for each hardware platform separately. The default number of tracks per basket used for these comparisons was 16.

**Table 15** The relative CPU performance of the GeantV single track mode, *GV-strk*, which emulates Geant4-style tracking, compared with the default GeantV basketized mode, *GV-bskt*.

Processor	GV-bskt	GV-strk	GV-strk/GV-bskt
Intel E2620	2621 sec	2960 sec	1.13
Intel E2680	1628 sec	1533 sec	0.94
AMD 6128	4457 sec	4817 sec	1.08

## 6.3 Profiling analysis

We present detailed profiling information illustrating the relative performance of different components (geometry, physics and magnetic field propagation) along with the major hotspots. Results are compared with Geant4 to understand which components exhibit different performance features. We also present these profiles for different configurations of the CMS application by varying the cuts and for the simplified calorimeter example. Shown in Table 16, 17, 18 are lists of top 10 functions of GeantV for different configurations in terms of the exclusive CPU time while Tables 19 is the list of top CPU functions from the Geant4 application. In general, there are no unexpected hotspots or bottlenecks, which

indicates both GeantV and Geant4 applications are reasonably well modularized and granulated already. On the other hand, there exist noticeable differences between the scalar and the vector mode of GeantV. For example, the CPU fraction of `CMSmagField::EstimateFieldValues` is significantly reduced in the vector mode as it is efficiently vectorized. Note that the overhead from the geometry basketization is largely due to the extra track handling such as `Handler::AddTrack` and `Handler::Flush` which are shown in Table 17, but not in Table 18. It is also worthwhile to note that `Spline::GetValueAt` of GeantV takes significantly less time than its equivalent function of Geant4, `G4PhysicsVector::Value` which is the top CPU function of recent versions of Geant4.

**Table 16** Top-10 functions of the GeantV scalar mode.

% time	Function name
8.22	<code>CMSmagField::EstimateFieldValues</code>
5.44	<code>ScalarNavInterfaceVGM::NavIsSameLocation</code>
5.36	<code>DormandPrinceRK45::StepWithErrorEstimate</code>
3.32	<code>SimpleABBoxLevelLocator::LevelLocate</code>
2.99	<code>__GI_memcpy</code>
2.98	<code>SimulationStage::Process</code>
2.87	<code>PhysicsProcess::PostStepLimitationLength</code>
2.75	<code>Spline::GetValueAt</code>
2.25	<code>GSMSCModel::ComputeParameters</code>
2.19	<code>HybridNavigator::GetHitCandidates_v</code>

**Table 17** Top-10 functions of the GeantV vector mode.

% time	Function name
5.45	<code>ScalarNavInterfaceVGM::NavIsSameLocation</code>
4.95	<code>Handler::AddTrack</code>
4.66	<code>Handler::Flush</code>
4.32	<code>CMSmagField::EstimateFieldValues</code>
3.44	<code>SimulationStage::CopyToFollowUps</code>
3.13	<code>SimpleABBoxLevelLocator::LevelLocate</code>
2.78	<code>SimulationStage::Process</code>
2.78	<code>PhysicsProcess::PostStepLimitationLength</code>
2.55	<code>memcpy</code>
2.48	<code>GeomQueryHandler::DoIt</code>

## 6.4 Vectorization performance

We compared performance when switching on/off basketization per component. We enabled a mode allowing the grouping of baskets of tracks, but with dispatch in scalar mode, that allowed the evaluation of the overheads of basketization.

**Table 18** Top-10 functions of the GeantV vector mode except Geometry.

% time	Function name
6.68	<code>ScalarNavInterfaceVGM::NavIsSameLocation</code>
4.84	<code>CMSmagField::EstimateFieldValues</code>
4.17	<code>SimpleABBoxLevelLocator::LevelLocate</code>
3.56	<code>SimulationStage::Process</code>
3.11	<code>PhysicsProcess::PostStepLimitationLength</code>
2.86	<code>memcpy (libc-2.12.so)</code>
2.74	<code>HybridNavigator::GetHitCandidates_v</code>
2.68	<code>Spline::GetValueAt</code>
2.56	<code>SimulationStage::CopyToFollowUps</code>
2.47	<code>DormandPrince5RK::StepWithErrorEstimate</code>

**Table 19** Top-10 functions of the Geant4.

% time	Function name
6.52	<code>G4PhysicsVector::Value</code>
5.20	<code>G4ScalarRZMagFieldFromMap::GetFieldValue</code>
3.36	<code>G4Navigator::LocateGlobalPointAndSetup</code>
2.52	<code>G4DormandPrince745::Stepper</code>
2.38	<code>G4Navigator::ComputeStep</code>
2.36	<code>G4VEmProcess::PostStepGPIL</code>
1.92	<code>G4PropagatorInField::ComputeStep</code>
1.77	<code>G4Transportation::AlongStepGPIL</code>
1.67	<code>G4VoxelNavigation::ComputeStep</code>
1.64	<code>G4Mag_UsualEqRhs::EvaluateRhsGivenB</code>

Table 20 shows the fraction of vector instructions in each module of GeantV and the relative CPU gain introduced by vectorization with respect to the scalar mode for each of the enabled vectorization options. The CPU gain is relatively small, even though the fraction of vector instructions is significant. This is due to several factors including the basketization overheads (10-25% shown in in Appendix B), inefficiency from gather/scatter and mask operations in vectorization. In addition, the poor vector performance of geometry is not per se due to lack of vectorization, but to the execution of sequential algorithms used in navigation. Note that the sizable amount of vector instructions in scalar mode (15.67%) comes from compiler auto-vectorization and `VecGeom` internal vectorization.

## 6.5 Concurrency performance

We present the multi-threaded performance of the GeantV applications compared to the Geant4 equivalent, presenting scalability features and pros and cons for track-level parallelism versus event-level parallelism.

The strong scaling behavior of the GeantV prototype is shown in Fig. 22. The efficiency loss of about 25% when filling 16 physical cores is not ideal, and is due to

**Table 20** Vector instruction and the relative gain in CPU by vectorization of a specific module with respect to the scalar mode: The fraction of vector instructions,  $(\text{PAPL\_DP\_VEC})/(\text{PAPL\_DP\_OPS})$  where  $\text{PAPL\_DP\_OPS}$  and  $\text{PAPL\_DP\_VEC}$  are floating point (double precision) operations and double precision vector/SIMD instructions in 1-billion counters, respectively. MSC-vec is the case when vectorization in the GeantV multiple scattering (MSC) model is turned on. The Opt-vec is the same as All-vec, but Geom-vec is turned off.

Mode	PAPL_DP_OPS	PAPL_DP_VEC	%	Gain
Scalar	1770	277	15.67	-
Geom-vec	1771	333	18.82	0.96
Field-vec	1858	814	43.83	1.08
MSC-vec	1789	397	22.24	1.02
Phys-vec	1785	343	19.25	1.00
All-vec	1868	1051	56.26	1.00
Opt-vec	1868	996	53.35	1.12

both extra memory contention for shared track basketizers, and to basket efficiency decrease with increasing the number of threads.

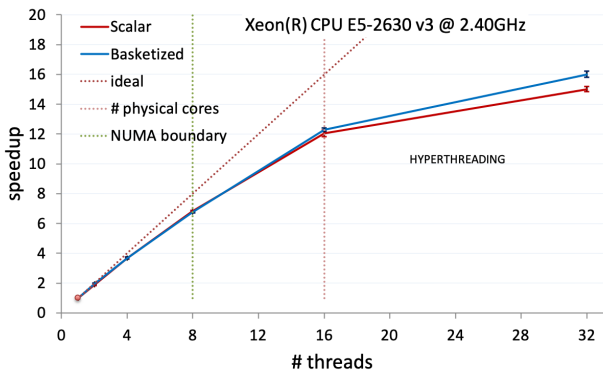


**Fig. 22** Strong scaling for the CMS example benchmark on a dual-socket Xeon(R) CPU E5-260 v3 @ 2.40 GHz having 8 cores per socket. The simulation was performed separately for scalar and basketized workflows.

Figure 23 shows the memory use versus the number of threads. As a general remark, the memory footprint is largely dominated by the number of tracks in flight. Increasing the number of threads requires more tracks for load-balancing, but the memory can be kept under control at the price of lowering the basket efficiency.

## 6.6 Performance in an experiment framework

The performance of GeantV is analyzed after integration into the CMS simulation framework as discussed in Sect. 5.2. In order to compare with Geant4, it is

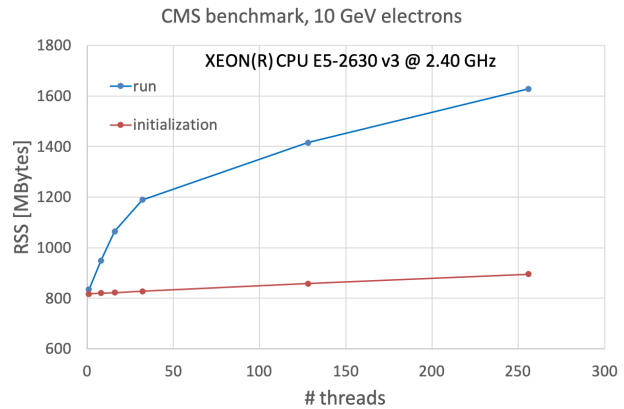


**Fig. 23** Memory efficiency for the CMS example benchmark on a dual-socket Xeon(R) CPU E5-260 v3 @ 2.40 GHz having 8 cores per socket.

necessary to configure the application as similarly as possible to the options available in GeantV. These settings include an EM-only physics list that supports the same models that have been vectorized in GeantV, as well as the same production cuts and other cuts. The same magnetic field integrator and stepper are used. The CMS detector geometry corresponds to the version operated in 2018. CMS has also introduced several optimizations to improve the CPU performance of the Geant4-based simulation, including Russian roulette and shower libraries [44, 45]; the optimizations that are not compatible with GeantV are disabled. There is good agreement in the physical output quantities from equivalent GeantV and Geant4 runs in the CMS software, validating the performance comparisons [46].

The tests are conducted using 500 generated events with two electrons, each at  $E = 50$  GeV, with random directions in  $\eta$  and  $\phi$ . A constant magnetic field of  $B = 3.8$  T is used. The CMSSW tests compare single-threaded to multi-threaded performance, as multi-threaded jobs are necessary for efficient use of the WLCG resources. To ensure a constant workload, the number of events per thread is kept constant in each test by reusing the initial 500 generated events. Unused threads are kept busy to simulate production conditions with all cores in use. The CPU and memory usage of the main program are estimated with output disabled, as the overhead from output is the same for Geant4 and GeantV. In the GeantV tests, vectorized algorithms are enabled for multiple scattering and magnetic field propagation. Both the basketized and single track modes of GeantV operation are tested.

Several different machines were used for the tests, with different cache sizes and other parameters. Table 21 summarizes the results. This table also includes results from the GeantV built-in standalone CMS test with sim-

ilar settings, in order to characterize the performance observed in the full CMSSW framework. There is virtually no difference in performance between basketized mode and single track mode. In all cases, the single thread speedup in CMSSW exceeds the single thread speedup from the standalone test. This is likely due to the additional instructions included when running in the CMSSW framework. The smaller instruction size from GeantV plays an even more important role in this case, as it allows more CMSSW instructions to be cached by the CPU. More pronounced speedups, along with more pronounced differences between CMSSW and the standalone, are seen in machines with smaller caches, supporting this explanation. Unfortunately, the speedup declines as the number of threads is increased, because GeantV does not scale as well as Geant4 with multiple threads. As expected, GeantV uses more memory than Geant4. For both programs, the memory usage increases linearly with the number of threads. Figures 24 and 25 depict the scaling behavior of throughput and memory for Geant4 and GeantV as the number of threads increases, using the E5-2683 v3 machine.

## 7 Lessons learned

The GeantV R&D project performed an in-depth investigation of alternative particle transport scheduling models for simulation. While the main objective was to achieve important speedups from vectorization and extra locality, there were several other direct or derived studies producing important results and conclusions. These are briefly discussed in the following subsections.

### 7.0.1 Vectorization model, basketization and parallelism

In order to take advantage of code that executes in using vector instructions, tracks that are similar needs to be gathered together and this introduces many significant challenges.

One challenge is the trade-off between memory use and efficiency. For example, we had to restrict the number of shapes for which we collected tracks into shape specific baskets to avoid memory explosions due both to the number of baskets and to the number of tracks in flight needed to fill those baskets. However, this means that only the shapes that are selected can benefit from vectorization.

Similarly, in order to fit within the user memory budget, we must limit the number of events in flight. In practice this means that when the number of tracks in flight for a given event starts to significantly ramp down, we need to close out this event so that we can start a new one and avoid starvation. To close out an event

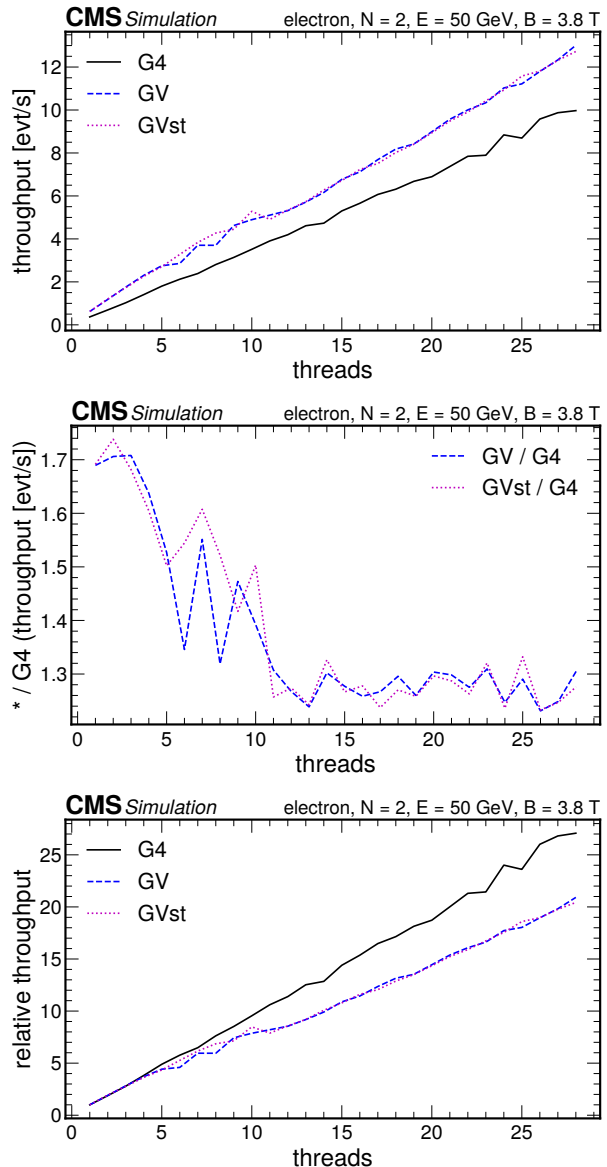


**Fig. 24** Top: throughput in events per second for Geant4 (black), GeantV (blue), and GeantV single track mode (purple). Middle: throughput ratio for Geant4/GeantV (blue) and Geant4/GeantV single track mode (purple). Bottom: speedup calculated as throughput(N threads) / throughput(1 thread). The E5-2683 v3 CPU was used for these tests.

is an expensive operation whose cost grows with the total number of baskets: one has to find all outstanding baskets that still have at least one track belonging to the event and close them out in scalar mode, since they have not reached the run-in-vector mode threshold. All these factors, plus the lack of vectorized navigation, means that the gains from vectorization of the geometry stage has been marginal at best, even-though the VecGeom primitives are amongst the best vectorized code.

When introducing multiple threads, load balancing becomes yet another challenge where synchronization

**Table 21** CMSSW test results with different machines, both single-threaded and multi-threaded. Standalone results are included as a comparison. Ratios of throughput (#events/s) and memory usage are both shown. The “N threads” column shows the result for the maximum number of threads (physical cores) for each machine. The cache value corresponds to the largest cache for each processor: L3 for the E5-2683 v3 and Gold 6248, and L2 for the E5-2660 v2.

Machine	Clock [GHz]	Cache [kB]	Cores	Throughput [GV/G4]			RSS memory [GV/G4]	
				Standalone 1 thread	1 thread CMSSW	N threads	1 thread CMSSW	N threads
E5-2683 v3	2.00	35840	28	1.60	1.69	1.30	1.56	2.34
Gold 6248	2.50	28160	20	1.49	1.66	1.18	1.54	2.31
E5-2660 v2	2.20	4096	8	2.14	2.63	2.18	1.42	2.36

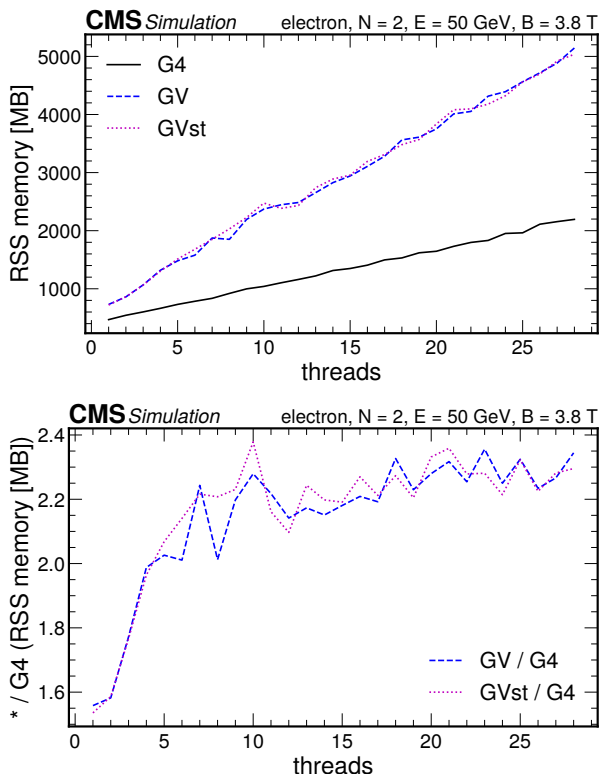


**Fig. 25** Top: RSS memory in megabytes for Geant4 (black), GeantV (blue), and GeantV single track mode (purple). Bottom: RSS memory ratio for Geant4/GeantV (blue) and Geant4/GeantV single track mode (purple). The E5-2683 v3 CPU was used for these tests.

points (however small they may be) are needed to determine how much of the work can and needs to be shared between threads and for the sharing itself. In order to increase scaling we have had to reduce several times the amount of sharing between threads at the expense of vector efficiency. An early versions was copying track data from one thread to another thread’s input stack essentially every time a track left a volume in order to go in to a volume of different type. In a later version, this happened only for tracks overflowing baskets when a different thread was idle (ran out of local tracks to process), and still the cost was noticeable, in particular

during event tails. In order to reduce contention on the shared resources, we also introduced the notion of a group of threads all pinned to a NUMA domain. Each group of threads was essentially independent of the others, with the tracks always staying within a single group. This arrangement also helps to reduce the amount of memory transfer across NUMA domains.

At first we assumed that we would benefit from gathering the memory fetches as close as possible. Even though we indeed saw improved CPU data cache usage in the implementation that passed the tracks from baskets to basket by copying the data, the real bottleneck, and major CPU time sink, was `memcpy` itself. We soon measured that the gain from avoiding `memcpy` was very large, even though it resulted in the access pattern to fill the vector register becoming much less efficient, due to a more fragmented data layout in memory. On the other hand, the cost of filling the vector register from this fragmented memory layout is noticeable and one of the major problems holding back any efficiency gain from vectorization.

### 7.0.2 Geometry

VecGeom library was one of the first software components put in place for GeantV and it helped to pave the way for GeantV as a whole as it lead to the development of VecCore, a framework for abstracting vector operations for different processor architectures, and demonstrating SIMD acceleration can be achieved in a portable manner. The programming model developed for VecGeom was generalized by introducing VecCore, which has been used in GeantV to write code that, with a single implementation, can be instantiated to support either scalar inputs or vector inputs. This model was not only used to improve the run-time performance of several algorithms with vector inputs, but also to improve the run-time performance of some algorithms even when the input is scalar. Which type of gain is more relevant depends strongly on the detector being simulated. It was also shown that automatic code generation and specialization of the algorithms, tailored to the target

geometry, can lead to significant further performance improvements.

### 7.0.3 Physics

Since the modeling of electromagnetic (EM) interactions of  $e^-$ ,  $e^+$  and  $\gamma$  particles with matter is the most intensively used and computationally-demanding part of most high-energy physics detector simulations, EM physics processes were selected to vectorize. Beyond vectorization, we first reviewed, overhauled and improved the existing code, based on an exhaustive review of the relevant literature. This resulted in optimized versions of the code that brought significant performance improvements to the physics code. Using model level tests to analyze the performance of the vectorized EM models over their (optimized) scalar versions, we achieved excellent  $\times 1.5$ - $3$  and  $\times 2$ - $4$  vectorization gains on Haswell and Skylake (AVX2) architectures, respectively. Unfortunately, these synthetic model test gains are not visible when integrating them into a full application that has to deal with the full collection of models, particle types and energies in a stochastic manner.

### 7.0.4 Magnetic field

The integration of the equations of motion of a charged particle in a non-uniform pure magnetic field (or an electromagnetic field) accounts for about 15–20% of the CPU time of a HEP application. After reengineering and vectorizing the implementation, we measured improvement in the ratio of the Geant4 run-time over the GeantV run-time in our yardstick example from a factor 1.88 in fully scalar mode to a factor 2.12 with the integration of the equations of motion implementation executed in vector mode.

### 7.0.5 Interfacing with user task-parallel frameworks

Concerning the ability to integrate the GeantV prototype in the experiments' simulation frameworks, two essential questions are whether the run-time performance gains are reproduced when the simulation is executed within the experiment framework and how much effort is needed to replace the simulation engine with the new implementation. We worked closely with the CMS experiment as they explored this integration to understand this better. During this co-development effort, we had several iterations on some of the fundamental features of the internal scheduler and its interfaces to order to ease the integration effort and improve run-time efficiency. Thanks to this collaboration, one of the results is the realization that integration of the prototype of

the GeantV toolkit within an experiment framework is relatively straightforward. The other major result is that the run-time performance gain seen in the standalone example is also seen in the integrated example, and is even slightly better.

## 8 Summary and conclusion

The GeantV R&D project has reached its conclusions after several years of development and study undertaken in the context of an international collaboration with the participation of the LHC experiments and under the umbrella of the HEP Software Foundation (HSF). Its main objective of demonstrating an achievable speedup of a novel approach based on parallel particle transport has been realised with the delivery of a prototype that simulates full electromagnetic showers in a realistic and complex calorimeter. It has been shown that the performance gain from the vectorization of the individual software components is largely lost in the process of reshuffling the particles for the vector operations. On the other hand, it has also been observed that significant improvements in the performance of the simulation software can be obtained by better exploitation of data and code locality, as well as through a more compact code based on modern programming idioms. These findings are informing the direction of future improvements of the Geant4 toolkit, including the investigation of architectural revisions.

Furthermore, the GeantV project has delivered the modular software packages VecGeom, VecCore and VecMath which are having a significant impact in different software areas within High Energy Physics. Those packages have already gone through all the phases of development, validation and integration, and are now used in production by toolkits like Geant4 and ROOT, and are delivering noticeable gains in performance.

In summary, the GeantV R&D project has contributed a set of useful libraries to the HEP software community, as well as valuable knowledge which has been used to set directions for further development of detector simulation toolkits. Future lines of work include modernization of the Geant4 simulation toolkit code, R&D for efficient utilization of accelerators in modern hardware platforms, as well as investigation of fast-simulation techniques which promise to provide the necessary speed and physics fidelity for utilization in a larger fraction of use-cases in future HEP experiments.

**Acknowledgements** This work was supported by Fermi Research Alliance, LLC under Contract No. DE-AC02-07CH11359 with the U.S. Department of Energy, Office of Science, Office of High Energy Physics. Part of this work

was supported by funds provided by Intel Corporation to the Center for Scientific Computing at the So Paulo State University under FUNDUNESP Grant No. 2323/2014. The authors would like to thank Graeme A Stewart (CERN) for his careful review of this article. We also owe a lot to many colleagues who supported the GeantV project and gave valuable feedback during the development period; Krzysztof Genser (Fermilab), Chris Jones (Fermilab).

## References

1. The HEP Software Foundation, A Roadmap for HEP Software and Computing R&D for the 2020s, *Computing and Software for Big Science*, vol. 3, p. 7 (2019)
2. S. Agostinelli *et al.*, GEANT4: A Simulation toolkit, *Nucl. Instr. Meth.*, vol. A506, pp. 250303 (2003)
3. A. Ferrari, P. R. Sala, A. Fassò, and J. Ranft, FLUKA: A multi-particle transport code (Program version 2005), CERN-2005-010, SLAC-R-773, INFN-TC-05-11 (2005)
4. R. Brun, R. Hagelberg, M. Hansroul, and J. Lassalle, Simulation program for particle physics experiments, GEANT: user guide and reference manual, Geneva: CERN (1978)
5. G. Amadio *et al.*, GeantV alpha release, *J. of Phys.: Conf. Ser.*, vol. 1085, p. 032037 (2018)
6. G. Amadio, P. Canal, D. Piparo, and S. Wenzel, Speeding up software with VecCore, *J. of Phys.: Conf. Ser.*, vol. 1085, p. 032034 (2018)
7. M. Kretz and V. Lindenstruth, Vc: A C++ library for explicit vectorization, *Software: Practice and Experience* (2011)
8. P. Karpiński and J. McDonald, A high-performance portable abstract interface for explicit SIMD vectorization, *Proc. of the 8th Int. Workshop on Progr. Models and Appl. for Multicores and Manycores, PMAM17, ACM*, (New York, NY, USA), pp. 2128 (2017)
9. CMS Collaboration, CMSSW, [software] <https://github.com/cms-sw/cmssw> (accessed on 2020-01-28) (2018)
10. M. Gayer *et al.*, New software library of geometrical primitives for modeling of solids used in Monte Carlo detector simulations, *J. of Phys.: Conf. Ser.*, vol. 396, p. 052035 (2012)
11. J. Apostolakis *et al.*, Towards a high performance geometry library for particle-detector simulations, *J. of Phys.: Conf. Ser.*, vol. 608, p. 012023 (2015)
12. J. Apostolakis *et al.*, A vectorization approach for multifaceted solids in VecGeom, *Eur. Phys. J. Web of Conf.*, vol. 214, p. 02025 (2019)
13. S. Wenzel and Y. Zhang, Accelerating navigation in the vecgeom geometry modeller, *J. of Phys.: Conf. Ser.*, vol. 898, p. 072032 (2017)
14. GDML manual, <http://lcgapp.cern.ch/project/simu/framework/GDML/doc/GDMLmanual.pdf>
15. Intel® Embree - High Performance Ray Tracing Kernels. <https://embree.github.io/> (accessed 2020-01-28).
16. I. Wald, S. Woop, C. Benthin, G. S. Johnson, and M. Ernst, Embree: A kernel framework for efficient cpu ray tracing, *ACM Trans. Graph.*, vol. 33, pp. 143:1143:8 (2014)
17. D. Piparo *et al.*, Speeding up HEP experiments software with a library of fast and auto-vectorisable mathematical functions, *J. Phys.: Conf. Ser.*, vol. 513, p. 052027 (2014)
18. P. LECuyer, R. Simard, E. Chen, and W. Kelton, An object-oriented random number package with many long streams and substreams, *Nucl. Instr. Meth.*, vol. 50, pp. 10731075 (2002)
19. J. K. Salmon, M. A. Moraes, R. O. Dror, and D. E. Shaw, Parallel random numbers: as easy as 1, 2, 3, *Proc. of 2011 Int. Conf. for High Perf. Comp., Networking, Storage and Analysis*, pp. 16:112 (2011)
20. K. Savvidy and G. Savvidy, The MIXMAX random number generator, *Comp. Phys. Comm.*, vol. 196, p. 161 (2015)
21. P. LECuyer, Combined multiple recursive random number generators, *Op. Research*, vol. 44, p. 816 (1996)
22. G. Marsaglia, DIEHARD: A batter of tests of randomness, <https://webhome.phy.duke.edu/~rgb/General/dieharder.php> (accessed 2020-01-29) (1996)
23. P. LECuyer and R. Simard, TestU01: A C library for empirical testing of random number generators, *ACM Trans. on Math. Soft.*, vol. 33, No.4 Article 22 (2007)
24. J. Allison *et al.*, Recent developments in Geant4, *Nucl. Instr. Meth. Phys. Res. A*, vol. 835, pp. 186225 (2016)
25. Geant4 Collaboration, Geant4 documentation: Guide for physics lists, <http://geant4-userdoc.web.cern.ch/geant4-userdoc/UsersGuides/PhysicsListGuide/html/index.html> (accessed 2020-01-28)
26. G. Amadio *et al.*, Electromagnetic physics vectorization in the GeantV transport framework, *EPJ Web Conf.*, vol. 214, p. 02031 (2019)
27. Google Benchmarks, A library to benchmark codesnippets, <https://github.com/google/benchmark> (accessed 2020-01-29)
28. A. Buckley, P. Ilten, D. Konstantinov, Lönnblad, Leif, J. Monk, W. Porkorski, T. Przedzinski, and A. Verbytskyi, The HepMC3 event record library for Monte Carlo event generators, arXiv:1912.08005 (2019)
29. R. Brun and F. Rademakers, ROOT: An objectoriented data analysis framework, *Nucl. Instr. Meth. A*, vol. 389, pp. 8186 (1997)
30. GeantV git: GeantV Git repository, <https://gitlab.cern.ch/GeantV/geant/tree/pre-beta-7> (accessed 2019-12-09)
31. J. H. Halton, Pseudo-random trees: Multiple independent sequence generators for parallel and branching computations, *J. of Comp. Phys.*, vol. 84, pp. 156 (1989)
32. H. G. Schaathun, Evaluation of splittable pseudo-random generators, *J. of Funct. Progr.*, vol. 26, e6 (2015)
33. C. E. Leiserson *et al.*, Deterministic parallel random-number generation for dynamic multi-threading platforms, *SIGPLAN Not.*, vol. 47, p. 193 (2012)
34. D. Savin, Using pseudo-random numbers repeatably in a fine-grain multithreaded simulation, <https://sd57.github.io/g4dprng/gsocPreprint.html>
35. D. V. Elvira, Readiness of the CMS detector simulation, *NSS/MIC 2007 C07-10-28*, vol. 3, pp. 20812085 (2007)
36. D. J. Lange, M. Hildreth, V. N. Ivantchenko, and I. Osborne, Upgrades for the CMS simulation, *J. Phys. Conf. Ser.*, vol. 608, no. 1, p. 012056 (2015)
37. M. Hildreth, V. Ivantchenko, and D. J. Lange, Upgrades for the CMS simulation, *J. Phys. Conf. Ser.*, vol. 898, no. 4, p. 042040 (2017)
38. Intel®, Thread Building Blocks, [software] <https://www.threadingbuildingblocks.org> (accessed 2020-01-28) (2018)
39. A. Bocci, D. Dagenhart, V. Innocente, M. Kortelainen, F. Pantaleo, and M. Rovere, Bringing heterogeneity to the CMS software framework, arXiv:2004.04334, Submitted to *Eur. Phys. J. Web Conf.* (2019)
40. M. Dobbs and J. B. Hansen, The HepMC C++ Monte Carlo event record for High Energy Physics, *Comput. Phys. Commun.*, vol. 134, pp. 4146 (2001)
41. K. Pedro and S. Banerjee, SimGVCORE, [software] <https://github.com/kpedro88/SimGVCORE> (accessed 2019-07-02) (2019)

42. D. Terpstra, H. Jagode, H. You, and J. Dongarra, Collecting performance data with PAPI-C, *Tools for High Perf. Comp. 2009*, pp. 157173 (2010)
43. Open|Speedshop, [software]<https://openspeedshop.org>
44. J. Apostolakis *et al.*, HEP Software Foundation Community White Paper Working Group - Detector Simulation. arXiv:1803.04165 (2018)
45. K. Pedro, Current and future performance of the CMS simulation, *Eur. Phys. J. Web Conf.*, vol. 214, p. 02036 (2019)
46. K. Pedro, Integration and performance of new technologies in the CMS simulation, arXiv:2004.02327, Submitted to *Eur. Phys. J. Web Conf.* (2019)

A Appendix 1: First versions of the GeantV scheduler

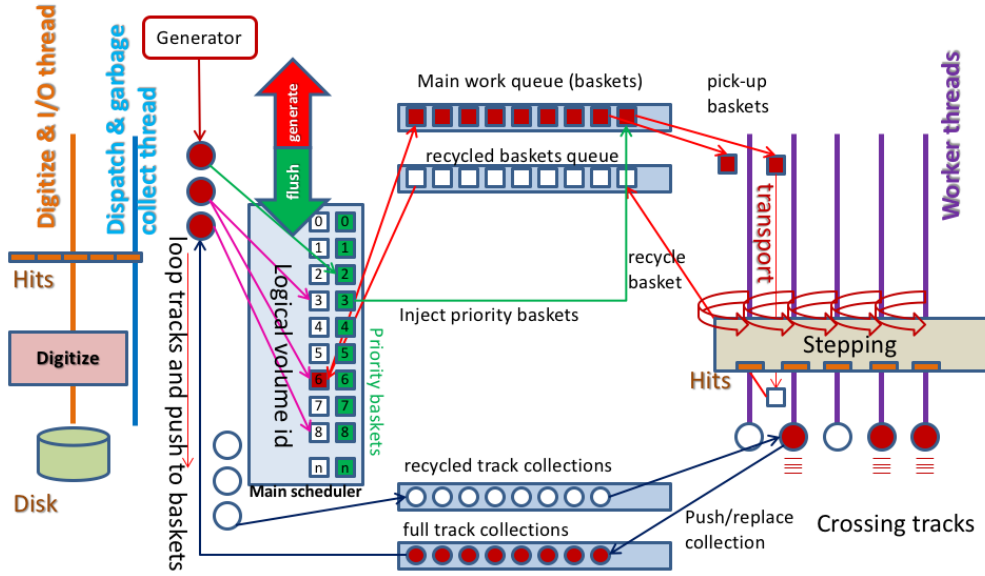


Fig. 26 First version of geometry-oriented GeantV scheduling. Besides the worker threads performing the transport, version 1 had a garbage collector thread and an I/O thread.

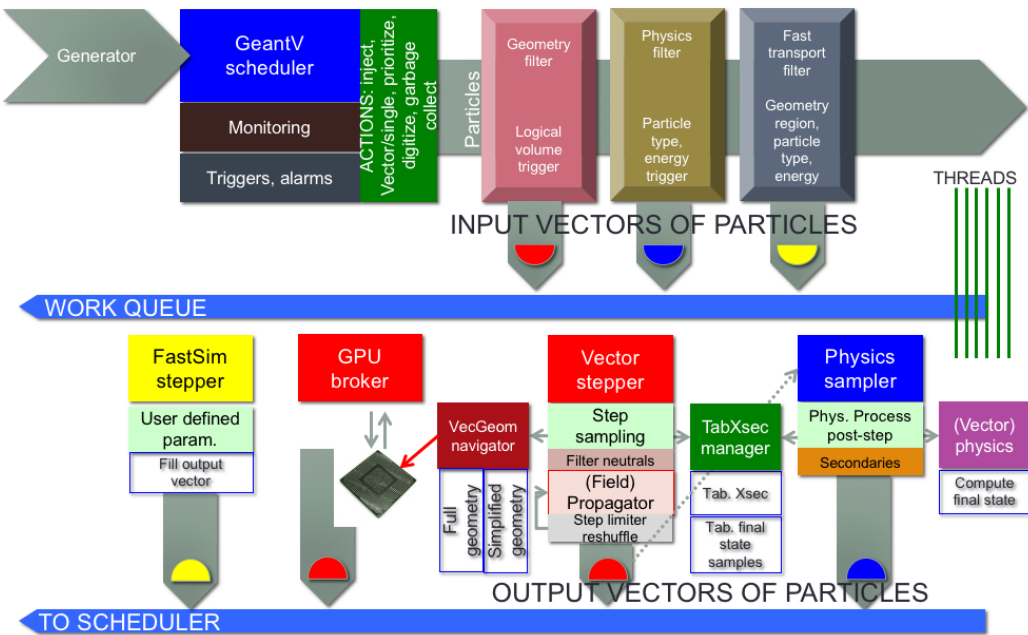


Fig. 27 Second version of GeantV scheduler. Track data was handled using a structure of arrays of aligned data. This version was able to handle simplified tabulated physics in addition to geometry and was NUMA-aware.

## B Appendix 2: Performance benchmark

Most of the multi-thread scaling and vectorization performance analysis was based on data collected using high-end machines, and the most relevant results have been described on Sect. 6. Another approach to performance analysis has been carried out, namely, a comparative study using several different, typical end-user machines, to collect performance data for a wide spectrum of machine specifications. The goal of using a more heterogeneous set of machines was to assess how lower-grade processors and low-memory conditions would affect the performance of the prototype.

The study was based on 1000 10-GeV single-electron events per job, through the GDML 2018 CMS model available from the GeantV repository. For Geant4, release 10.4.p03 in single-thread mode was the baseline configuration. To minimize external interference, jobs were submitted in exclusive-use conditions. Each job configuration was run ten times, and results are based on simple averages of CPU times.

Some of the performance numbers from different architectures are provided in the following tables. The first few columns describe details of each machine’s configuration used in this study, including processor, brand, operating system, memory and compiler version used. The last columns represent performance results, providing timing averages and uncertainty estimates.

Table B-21 shows global performance measurements. Absolute timing measurements in GV column roughly agree with processor power and clock speeds. The G4/GV ratio, directly comparing Geant4 with GeantV performances, ranges from 1.03 up 1.92 over different hardware platforms. GeantV in single-track processing mode (strk) shows some expected correlation with the G4/GV ratio. The vector gain shows best results for hardware with the best SIMD capabilities, but it also shows a low-level of vectorization density, probably due to the difficulty of vectorizing HEP simulations.

Table B-22 shows the basketization overheads, in an attempt to assess the performance costs attributable to packing the data for vectorization efficiency, but without the corresponding vectorization gains, for jobs where the vectorized algorithms had been explicitly disabled. The basketization process collects tracks with similar characteristics, in order to maximize the SIMD synchronization (e.g. vectorization efficiency), as described earlier.

The track basketization was done separately per simulation stages (magnetic-field propagation, physics, geometry, multiple scattering), as the requirements for each stage are different. The geometry basketization requirements are the most strict, since tracks need to be in the same logical (rather than physical) volume. This produces a very large number of baskets, as compared to the basketization requirements for other stages, corresponding to a very significant performance degradation. Ultimately, the most performant GeantV configuration had geometry basketization (and vectorization) disabled at job initialization level, which is shown at the **FPM** and **Vector gain** table columns.

Different machines present different constraints for the GeantV runtime environment, and the observed performance can show some of those aspects. Some trends can be observed, however a more precise interpretation of the effects from different parameters is hard to disentangle unambiguously from the final numbers.

**Table 22** Performance analysis by architecture. The **GV** column shows absolute timing in seconds for a scalar single-thread GeantV configuration, while all other columns provide speedups or ratios, as indicated, relative to this column. The **strk** stands for single-track GeantV mode. See text for more details.

CPU specs	OS	gcc	SIMD	L1 cache	L2 cache	L3 cache	GV [sec]	G4/GV	strk/GV0	Vector gain
Intel i7 2.5GHz	Ubuntu 16.04	5.4.0	AVX2	126KB	1MB	8MB	941 ± 5	1.41 ± 0.04	1.02 ± 0.02	1.09 ± 0.01
Intel Core i7-4510U 2GHz	Ubuntu 16.04	5.4.0	AVX	128KB	512KB	4MB	1303 ± 3	1.09 ± 0.01	0.95 ± 0.07	1.09 ± 0.08
AMD A10-7700k	Fedora Workstation 29	8.2.1	AVX	2x96 KB I, 4x16 KB D	2x2MB	-	1828 ± 5	1.80 ± 0.04	1.25 ± 0.03	1.01 ± 0.01
Intel Celeron 1000M 1.8GHz	Fedora Workstation 29	8.3.1	SSE4	64KB	512KB	2MB	2769 ± 10	1.03 ± 0.01	1.11 ± 0.01	0.84 ± 0.01
Intel Centrino 2	Fedora Workstation 29	8.2.1	AVX	-	2x2MB	-	2592 ± 2	1.92 ± 0.01	1.24 ± 0.01	1.01 ± 0.01

**Table 23** Basketization overhead study, by architecture.  $B_o$  is the basketization overhead of GeantV, which is measured separately for different stages, namely propagation in magnetic field, physics, geometry, multiple scattering (MSC) and combined field+physics+MSC (FPM). The latter configuration was shown to be the most performant configuration in the high-end, multi-threading machines, as shown on Sec.6. See text for more details.

CPU specs	gcc	SIMD	L1 cache	L2 cache	L3 cache	$B_o$ (B-field)	$B_o$ (phys)	$B_o$ (geom)	$B_o$ (MSC)	$B_o$ (FPM)
Intel i7 2.5GHz	5.4.0	AVX2	128KB	1MB	8MB	2% ± 1%	2% ± 1%	6% ± 1%	0% ± 1%	3% ± 1%
Intel Core i7-4510U 2GHz	5.4.0	AVX	128KB	512KB	4MB	-1% ± 7%	-3% ± 7%	12% ± 9%	-4% ± 8%	2% ± 8%
AMD A10-7700k	8.2.1	AVX	2x96 KB I, 4x16 KB D	2x2MB	-	15% ± 1%	4% ± 1%	15% ± 1%	1% ± 1%	13% ± 1%
Intel Celeron 1000M 1.8GHz	8.3.1	SSE4	64KB	512KB	2MB	9% ± 1%	5% ± 1%	9% ± 1%	-1% ± 1%	9% ± 1%
Intel Centrino 2	8.2.1	AVX	-	2x2MB	-	6% ± 1%	3% ± 1%	13% ± 1%	-1% ± 1%	7% ± 1%
AMD e-300	8.2.0	SSE2	64KB	1MB	-	1% ± 1%	3% ± 1%	-3% ± 1%	-2% ± 1%	-